LAWRENCE
LIVERMORE
NATIONAL
LABORATORY

LLNL-TR-408722

LIFE Target Fabrication Research Plan Sept 2008

R. Miles, J. Biener, S. Kucheyev, R. Montesanti, J. Satcher, C. Spadaccini, K. Rose, M. Wang, A. Hamza, N. Alexander, L. Brown, J. Hund, R. Petzoldt, W. Sweet, D. Goodin

November 14, 2008

Disclaimer

This work performed under the auspices of the U.S. Department of Energy by Lawrence Livermore National Laboratory under Contract DE-AC52-07NA27344.

LIFE Target Fabrication Research Plan
Sept 2008

LLNL Contributors: Robin Miles, Juergen Biener, Sergei Kucheyev, Rick Montesanti, Joe Satcher, Chris Spadaccini, Klint Rose, Morris Wang, Alex Hamza

General Atomics Contributors: Neil Alexander, Lloyd Brown, Jared Hund, Ron Petzoldt, Wendi Sweet, Dan Goodin

Rev: 11/6/2008

Table of Contents

1.0 Executive Summary

The target-system for the baseline LIFE fast-ignition target was analyzed to establish a preliminary estimate for the costs and complexities involved in demonstrating the technologies needed to build a prototype LIFE plant. The baseline fast-ignition target upon which this analysis was developed is shown in Figure 1.0-1 below. The LIFE target-system incorporates requirements for low-cost, high throughput manufacture, high-speed, high accuracy injection of the target into the chamber, production of sufficient energy from implosion and recovery and recycle of the imploded target material residue. None of these functions has been demonstrated to date. Existing target fabrication techniques which lead to current "hot spot" target costs of ~$100,000 per target and at a production rate of 2/day are unacceptable for the LIFE program. Fabrication techniques normally used for low-cost, low accuracy consumer products such as toys must be adapted to the high-accuracy LIFE target. This will be challenge. A research program resulting is the demonstration of the target-cycle technologies needed for a prototype LIFE reactor is expected to cost ~$51M over the course of 5 years. The effort will result in targets which will cost an estimated $0.23/target at a rep-rate of 20 Hz or about 1.73M targets/day.

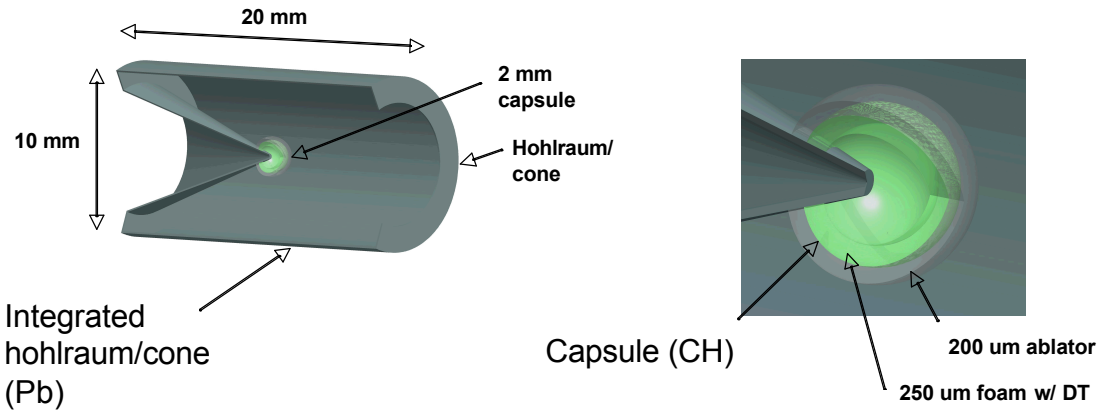

Figure 1.0-1 *Baseline LIFE fast-ignition target*

2.0 Introduction

At the heart of the LIFE system is a tiny amount of solid DT which is compressed by an intense energy pulse until a fusion reaction is initiated. The fusion reaction creates a neutron flux sufficient to cause a fission reaction in pellets flowing through the surrounding chamber walls. The fission reaction produces thermal energy for electricity generation. The target which houses the DT consists of a spherical capsule with an internal layer of foam which retains the DT within its pores. The capsule is attached to the hohlraum which converts laser light into x-ray energy to compress the DT and a cone which injects energy directly in the center of the imploding capsule to hasten the fusion reaction. Prior to implosion, the candidate fast-ignition LIFE target shown in Figure 1.0-1 is fabricated in a factory adjacent to the LIFE reactor and is injected into the target chamber at a rate of 13 to 20 targets per second. Following implosion, the residual target material must be removed from the chamber walls and pumps which constantly refresh the chamber's xenon atmosphere. A schematic showing the lifecycle of the targets is shown in Figure 2.0-1.

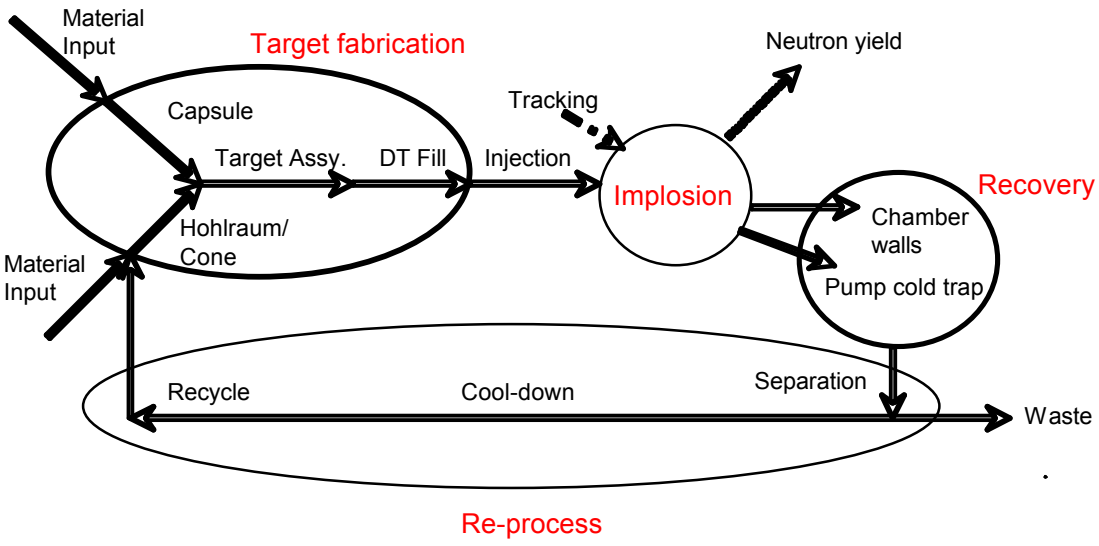

Figure 2.0-1 *Target Life-cycle*

The maximum allowable cost of the targets is driven by the anticipated cost of energy and the rate of target consumption. Using today's cost of energy and a consumption rate of 13 to 20 targets per second or about 1.73M targets/day, the maximum allowable per-target cost is on the order of 25 to 50 cents. Technical requirements for the target include not only the ability to produce the required neutron/energy yield but also the ability to be injected into the chamber without damage, tracked to determine its trajectory for final laser alignment and consist of materials which are retrievable and recyclable if necessary following implosion. A target meeting these objectives has not yet been fully designed but it is generally thought that such a target will consist of a limited set of materials and

will be produced using techniques associated with consumer-oriented low-cost, high throughput factories.

The "base-line" fast ignition target shown in Figure 1.0-1 is comprised of a capsule roughly 2.3 mm in outer diameter with a roughly 200 um wall thickness and 250 um foam thickness. The hohlraum in which the capsule sits is about 20 mm in length and about 10 mm inner diameter with a 250 to 500 um wall thickness and features a cone on one end which penetrates the capsule to facilitate injection of energy directly into the capsule center. The cone window at its apex is 10 um thick. Additional preliminary specifications are listed in Table 2.0-1. The hohlraum and the cone are high-Z materials while the capsule and internal foam which defines the DT layer are low-Z materials. Lead is a good candidate material for the hohlraum and cone because it is inexpensive, easily formable for good manufacturability and is recyclable after 2 years of storage following implosion-induced activation. Possible concerns with using lead as target material include corrosion of the chamber walls by the liquid lead following implosion and the low electrical conductivity if induction-based injection is used.

Table 2.0-1 *LIFE target specifications*

Component	Nom. Dim	Min. Dim.	Max. Dim.	Dim. Tol.	Surface Fin.
Hohlraum					
Diameter(ID)	10 mm			10 um	
Length (Inner)	20 mm				
Thick	200 um	20 um	500um	10 um	
LEH	70%				
Cone					
Angle	40 deg				
Thick					
Apex thickness	10 um				
Capsule					
Diameter (OD)	2.3 mm			+- 10 um	<100 nm RMS
Thickness	200 um			+- 5 um	
OOR				< 0.1%	
Foam thickness	250 um			+- 20 um	
Foam density	30 mg/cc				

At this point in time, the LIFE target is not yet fully designed nor have the target fabrication, injection, tracking and material recovery and recycling issues been resolved. Previous targets and those planned to be used at NIF have been made using precision machining techniques and hand-assembly at production rates of at most 2 per day and at costs of several tens of thousand dollars per article. The current target designed for the National Ignition Campaign (NIC) is a "hot spot" target with specifications expected to be an order of magnitude more precise in terms of capsule uniformity and surface finish than the fast ignition design. The majority of the current target fabrication techniques are unsuitable for low-cost, high throughput consumer items. A critical aspect of this effort

will be either the adaptation of current high-throughput manufacturing methods such as injection molding to the small but ultra-high precision needed for the LIFE targets and/or the development of new processes based on chemical engineering mass-production principles. The challenge in both cases is to determine whether or not inexpensive processes can be used to meet the specified tolerances of the LIF targets. The greatest probability of success lies with simple target designs using a minimal number of parts and materials that accommodate the component fabrication and assembly operations. Tolerances should, of course, be as generous as possible to facilitate cost-effective fabrication. Further, consideration of all aspects of the target lifecycle including injection and material recycling while meeting neutron/energy yield and cost constraints is paramount to overall system success. The final target design will be result of an optimization effort in which all factors are weighed and new solutions are explored to improve the overall target cycle.

This report outlines the requirements, current state-of-the-art and research plan for several aspects of the target life-cycle including target fabrication, injection and material recovery and recycle. Target design discussions are the subject of other reports. A significant research and development program is required to ultimately produce the LIFE targets to the desired specifications, costs, and production volumes.

3.0 Target Fabrication

Introduction

The primary objective of the target fabrication effort is to meet the cost, throughput and design specification requirements of the LIFE target. Unlike targets built to date, the LIFE target is not a research tool but is a key component in a commercial enterprise and must be cost competitive in the consumer market. At the current cost-point of $0.25/target, the cost per target is equivalent to the cost of making four Lego blocks at the current production cost of 6 cents per Lego block. At a rep-rate of 20 Hz, 1.73M targets per day will be manufactured and consumed. It is therefore natural to first consider manufacturing processes commonly used to make cost-competitive consumer products and to attempt to apply them to the process of target fabrication. These techniques include molding, stamping, emulsions and the like. Where these methods fail to satisfy cost or quality objectives, alternative processes may be developed and implemented. Because of the high degree of technical risk associated with qualifying these methodologies in a short period of time (< 10 years), a prudent research plan will pursue multiple paths simultaneously and trim them over time as objectives are met. In that vein, many fabrication techniques are suggested which are able to make at least one of the target components. For example, metal working techniques will likely be used for the hohlraum but might also be used for a beryllium capsule. Included in this section is information about development cost and schedule.

Overall process flow

There are many methods available for fabricating each of the major components of the target, the hohlraum/cone, the capsule and the foam. The fabrication options for each of these components is shown in Figure 3.0-1 below. None of these techniques have been qualified for high-volume target production and validation of these techniques for this application will be the subject of a research program. A discussion of each of these techniques can be seen in the subsequent sections of this report. Topics include fabrication techniques such as metalworking, injection molding, micro-encapsulation and others. As these techniques are implemented some will naturally be discarded in favor of others. Once a set of fabrication techniques are selected, a process flow diagram such as the one shown in Figure 3.0-2 will be constructed to illustrate the flow of material through the manufacturing line.

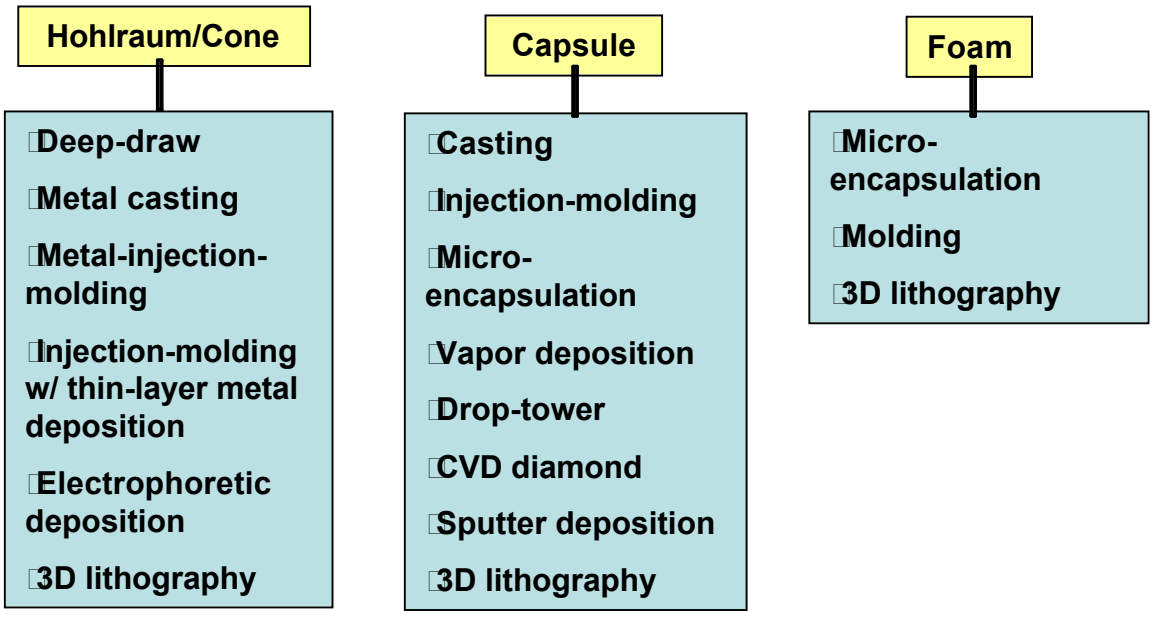

Figure 3.0-1 *Fabrication options for target components*

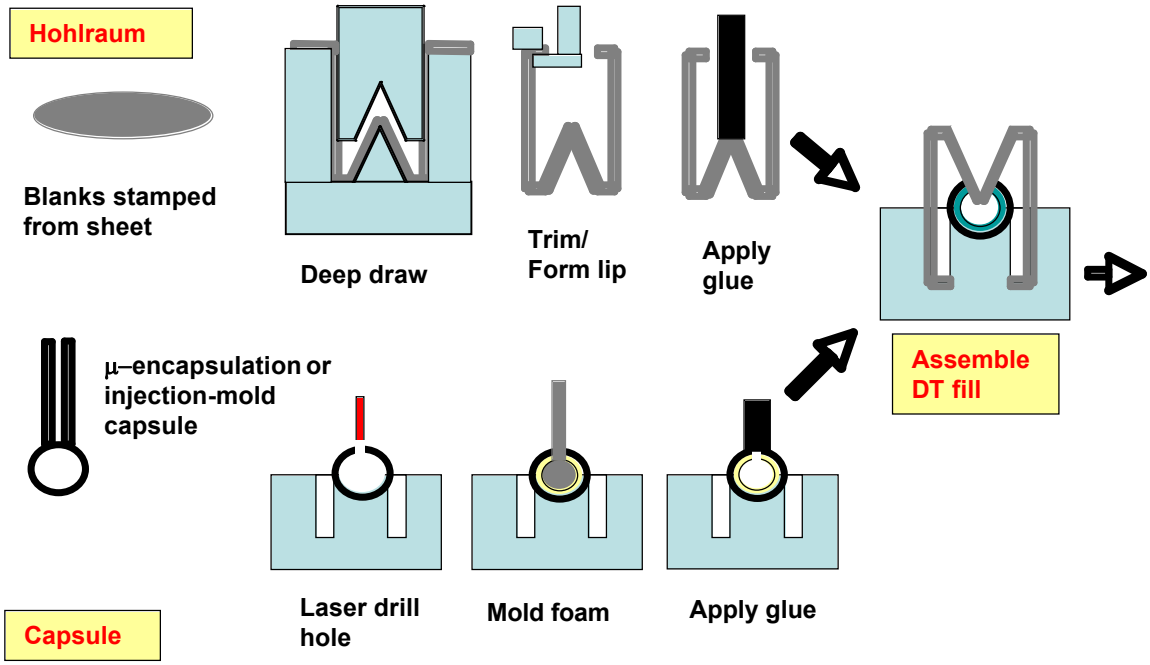

Figure 3.0-2 *Example target fabrication process schedule*

3.1 Metal working

3.1.1 Description and specifications

Metal working is a well-known metallurgical process that has been applied to form many metal components in our daily life. Historically, metal working technology can be divided into forming, cutting, and joining processes. Aluminum cans, for example are made through a deep draw process wherein blanks are first punched out of sheet metal stock. The blanks are then formed over tooling to shape the metal, rings are pulled around the outer diameter to further shape the metal to conform to the tooling, and the rim is trimmed and prepared to roll over the perimeter of the round top that has been previously stamped out of a separate metal sheet. Some metal parts are cast in molds in which the molten metal is poured. Upon cooling, the parts are released from the mold. Bullets are typically made using cast and formed pieces.

Due to its versatility, some metal working processes are desirable for:

1. One-step formation of smooth, robust, and uniform hohlraums and cones. Hohlraum and cones can be deep drawn around tooling which conforms the desired shape. Indentations for corner-cube reflectors for tracking can be punched into the surface of the hohlraums.
2. Metal capsules can possibly be cast or formed into hemispheres which are then joined to make the spherical capsules.
3. Joining of hohlraum and cone if necessary. Metal joint techniques such as brazing or welding can be considered for joining parts of the target.

The current specifications of hohlraum/cone are listed in section 2.0. The metal work must hold to the specified tolerances. Any extra material resulting from mold parting lines or joint operations must be removed.

3.1.2 Material Considerations

Current materials under consideration for the hohlraum/cone fabrication include gold, tantalum, lead, uranium, mercury, and bismuth, amongst which gold and lead are two top candidates for metal-working because of their good formability/workability at relatively low homogonous temperatures. Elemental lead, in particular, has unique advantages over other material systems because it is cost-effective, and amenable to large deformation processes such as deep drawing or stamping. Other material properties that must be taken into account when selecting hohlraum/cone materials include:

1. Mechanical properties (namely, strength and ductility), which determine the workability/formability of the selected metals. In general, low strength and good ductility are desirable for metal forming purpose.

2. The recrystallization and melting temperature of the metals. The low melting temperature metals allow cold-work or casting to be performed at low homogonous temperatures. This helps to save energy cost.
3. Strain hardening behavior of the metals. Too low or too high strain hardening ability of the metals leads to softening or early cracking, which are detrimental to metal working.
4. Cryogenic mechanical properties of the metals. This is important as hohlraum could be operated at low temperatures.
5. Weldability of the metals, if hohlraum and cone have to be assembled.

3.1.3 Current state of the art

Precision casting

Precision casting is a common technique to form auto parts and airplane components in the metallurgical industry. Compared with other metal-forming technologies, precision casting has some unique advantages:

1. It is good for small components/parts.
2. It exhibits excellent dimensional accuracy. The typical accuracy is 0.005 in. for the first inch, and 0.002 in. for each additional inch. Precision as high as 0.0002" (5 um) can be reached in Ultracast case.[1]
3. Features relatively smooth cast surfaces (1-2.5 μm RMS).
4. It can be used to cost very thin wall components (approximately 0.75 mm).
5. Suitable for complex shape components.
6. Allows massive production if sets of dies are applied.

The disadvantages of precision casting include:

1. High initial cost. Precision dies can be expensive.
2. High energy cost, as the materials have to be melted at high temperatures.
3. A certain account of porosity is common even though this problem can be alleviated by pressure-casting. It is unclear at present whether and how the porosity could affect the performance of the hohlraum. More specifications are needed.

Swaging/deep drawing

Swaging/deep drawing is a metal-forging technique in which the dimension and shape of a target product is manufactured by forcing it into a preset die. The swaging/deep drawing process is performed at room or elevated temperatures, and thus requires that the target metal be malleable. Some unique advantages of swaging/drawing process include:

1. It is a room-temperature forging technique and thus save energy cost.
2. On average, swaging products have good surface finish and uniform wall thickness, making it particularly attractive for hohlraum fabrication. Wall thickness as low as 15μm can be achieved.

3. It can be used for massive productions.
4. It can have high precision and relatively low cost. Precision in the range of 2-4 μm is common. [2-5]

Some disadvantages of the swaging process include:

1. It's high initial cost, mainly equipment and die cost, similar to precision casting.
2. The swaging process is limited to relatively simple geometry components.
3. It is only good for ductile metals with proper strain hardening coefficient. This suggests that swaging process may not be applicable to brittle metals such as polycrystalline tungsten.
4. Product dimensions are in the millimeter size range. Scale-down could become expensive.

3.1.4 Throughputs and costs

1. Hohlraum material cost (assuming lead): 0.01 cents/target.
2. Throughput: 30,000/day (1 target / 3 seconds).
3. Capital equipment cost: TBD.
4. Die cost (equivalent to the capital equipment cost): TBD.
5. Energy cost (electricity): < material cost.
6. Plus manpower and space charge.

3.1.5 Research needs

The general scheme of the hohlraum fabrication requires our in-depth knowledge in metal-working that could be beyond the conventional structure-property region. As the hohlraum dimension approaches micrometer-sized region, the length scale that controls the material properties is often in the nanometer range where the materials properties are not well understood. On the other hand, the sample dimensions produced by the current state-of-the-art approaches described above are slightly larger than those required for hohlraums. Therefore, scale-down could become one of the major obstacles that we have to overcome in order to adopt the existing metal-working technologies. Our short- and long-term research needs include:

1. Specification clarification and material selection clarification.
2. Characterization of mechanical properties of the selected materials at various grain sizes and different temperatures (strength, ductility, fracture toughness, workability, etc.)
3. Characterization of other physical properties relevant to metal working including thermal expansion, viscosity of melted liquid, alloying effect, etc.
4. Investigation of recrystallization and work hardening behavior. These properties are important for metal working.
5. Determination of residual stress and texture after deformation. This will help us to understand the uniformity of the hohlraum walls.

6. Determination of weldability of the materials if the hohlraum and cone have to be assembled.
7. Consideration of alternative technologies other than metal-working. For example, using plastic (CH) hohlraum with coated metal layers.

Key research issues:

1) Scale-down of the current metal-working technologies for extremely small components.
2) Characterize the mechanical properties of hohlraum materials at micro- and nano-scale.

Research timeline for hohlraum/cone fabrication:

	FY 09	FY 10	FY 11	FY 12	FY 13
Hohlraum/cone materials selection	←	→			
Specs clarification (wall uniformality,alignment,voids etc.)	←	→			
Alternative technologies	←	→			
Scale-down of the current technology	←	→			
Mechanical properties at nanoscale and/or cryogenic temperatures, working hardening behavior, texture etc.		←	→	→	→
Other physical properties (thermal conductance, viscosity, etc.)		←	→	→	→

References:

1. http:// www. jobshop.com/techinfo/papers/tinyparts.shtml
2. http:// www. evanstechnology.com/qs_quality.html
3. http:// www. braxtonmfg.com/parts.html
4. http:// www. hobsonmotzer.com/about/
5. http:// www. oceyelet.com/products.htm

3.2 Injection molding

Micro-injection molding is one of the promising methods that could allow one to produce large quantities of high precision targets for the LIFE application at low costs. The technique is a special case of injection molding which is widely used in industry. This high-throughput, low-cost technology permits a high degree of process automation, and allows one to produce complex, precision parts from plastics, ceramics, and metals. Thus this technique could be potentially used to make both components of a LIFE target, the low-Z capsule as well as the high-Z hohlraum. To evaluate this technique for the LIFE target application we consulted *Nano- and Microsystem*s from *Forschungszentrum Karlsruhe*, Germany for their expert advice.

3.2.1 Description of micro injection molding

\The parts are formed by injecting molten plastic at high pressure into a heated and frequently evacuated mold, which is the inverse of the product's shape. Such mold inserts may be manufactured by mechanical micromachining (microcutting), laser micromachining, X-ray or UV lithography or by combinations of these and other processes. Depending on the component to be molded, the injection molding process is conducted isothermally or variothermally, i.e. with heating prior to injection and cooling prior to demolding. After cooling and opening of the tool, the injection-molded components are removed by a handling device/robot. Both cycle time and capital investment depend strongly on the actual process. In general, variotherm injection molding is slower and the capital equipment costs are higher but the process achieves better accuracy and reduces internal stresses of the polymeric material.

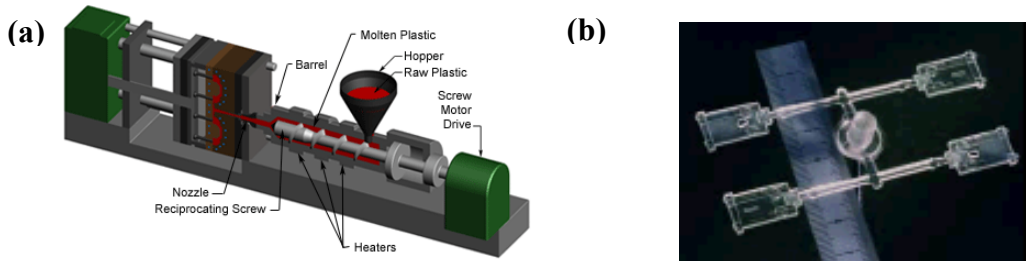

Figure 3.2.1-1 *(a) injection molding machine, and (b) a typical example of an injection-molded part (fiber connectors as removed from the tool using a 4 cavity mold).*

3.2.2 Current state of the art

Key technical data of current state-of-the-art injection molding are listed in table 3.2.2-1:

Table 3.2.2-1*: Technical data of the art injection molding*

Injection molding: technical data	
Preferred area of application	Fabrication of medium up to large series
Typical cycle time	< 15 s – 8 min
Smallest structural detail molded	≤ 200 nm

Roughness Ra	down to below 50 nm, depending on the type of mold insert
Highest aspect ratio reached so far: Free-standing structure (pin, web) Buried structure (hole, channel)	 17 (h=2000 μm, b=115 μm) 25 (h=250 μm, b=10 μm)
Materials	Nearly all thermoplastics and thermoplastic elastomers, elastomers and duromers are under development

The ablator capsule could be made from nearly all thermoplastics including polyethylene (PE). Hollow parts as the ablator capsule can be realized by gas-assisted injection molding. At present, it can not be said if this technique would be capable of delivering the required capsule wall thickness homogeneity (peak-to-valley roughness ~ 1% of the wall thickness, or <1 micron for a 100 micron thick ablator) as the fabrication of such high-precision mm-sized shells has not been demonstrated yet. Another issue is the formation of a seam (or burr) around the shell, which is the consequence of the two-part mold required for this process. Using a high precision mold one could expect a 5 micron wide and 5 micron high seam. Simulations need to be performed to address the effect of such a 2D line defect on target performance. To improve the ablation properties, one could potentially increase the density of the capsule material (PE ~ 1g/cc) by adding graphite (2.2 g/cc) or diamond nanoparticles (3.5 g/cc). Again, this is not a standard process, and would require R&D.

In a first order cost approximation, the material costs of the polymer can be neglected (even at a market price of $ 2000 per ton PE, an ablator shell costs only $2x10^{-4}$ cts). However, the capital equipment cost can be substantial. Depending on actual process requirements, an injection molding system can cost anywhere between $100,000–$500,000. The cycle time (filling time + cooling time + cycle reset) is typically in the order of a few seconds. Assuming a cycle time of 10 s ($3x10^6$ cycles/year) and further assuming a ten cavity mold, one would need 20 injection molding systems to fabricate the required $6x10^8$ pieces per year. Thus the upper limit of the of capital equipment depreciation costs (7 years/linear, $500,000 per injection molding system, 10 cavities per mold) would be in the order of 0.2 cts per piece.

In principle, the hohlraum structure could also be formed by injection molding using an organic binder highly filled with a high-Z metal powder (metal injection molding, MIM), followed by debinding and sintering. Although the parts typically ***shrink*** 15 to 20 percent during debinding and sintering, tolerances as low as 0.3% of the nominal dimension can be achieved. However, this technique has not yet been demonstrated for lead which is our preferred hohlraum material. In conclusion, metal injection molding might be an interesting alternative to the fabrication of the hohlraum by cold working (swaging, deep drawing) or casting, specifically in the case of high melting point and/or brittle materials such as tungsten.

3.2.3 Research Needs

Although both the low-Z ablator capsule and the high-Z hohlraum can in principle be fabricated by micro-injection molding techniques, it can not be said at present if the required precision can be achieved (e.g. in the case of the ablator capsule a wall thickness homogeneity of better than 1% of the wall thickness). Thus demonstrating that the required precision can be achieved will be the main obstacle that we have to overcome in order to adopt the existing injection molding technologies. Our short- and long-term research needs include:

1) Evaluation if the required precision can be achieved by a standard state-of-the-art micro-injection molding process
2) Perform simulations to assess the effect of defects inherent to the micro-injection molding process (such a seam around the shell) on target performance
3) Modification of micro-injection molding processes for improved precision
4) Development of a high-density plastic precursor (nanographite or nanodiamond doped plastic) for the ablator application
5) Development of a lead MIM process for the hohlraum application

3.2.4 Research timeline and costs

Table 3.2.4-1: *Proposed research timeline and costs associated with development of the micro-injection molding technique*

	FY 09	FY 10	FY 11	FY 12	FY 13
Evaluate current technology	←	—			
Develop ultra-high precision micro-injection molding	←	—	—		
Develop a high-density plastic		←	—		
Develop a lead MIM process			←	—	
Perform simulations on defects	←	—	—	→	
Demonstrate production				←	— →
Costs	$600k	$800k	$800k	$1000k	$1000k

3.2.5 Conclusion

Micro injection molding is a promising method that could allow one to produce large quantities of high precision targets for the LIFE application at low costs. It is a high-throughput, low-cost technology which permits a high degree of process automation, and potentially can be used to produce large quantities of both components of a LIFE target, the low-Z capsule as well as the high-Z hohlraum. However, at present it can not be said whether or not the required precision can be achieved.

3.3 Micro-encapsulation

3.3.1 Description and specifications

Microencapsulation is the general term given to the basic technique currently used in the fabrication of hollow spherical shells for ICF targets. A triple orifice generator is used, consisting of a concentric nozzle dispensing two immiscible liquids. (Figure 3.3.1-1) The inner liquid (oil 1) forms the inner void of a hollow shell, while the middle liquid (R/F) contains the precursor materials to form the shell wall. The outermost liquid is used to strip the droplet off of the tip of the nozzle into a collection tube. After formation of the compound droplet, the shell wall is cured into a solid and finally the liquid is extracted from the inside of the shell. For foam shells, an additional step is used to prepare a solid density plastic permeation barrier on the outside of the shell.

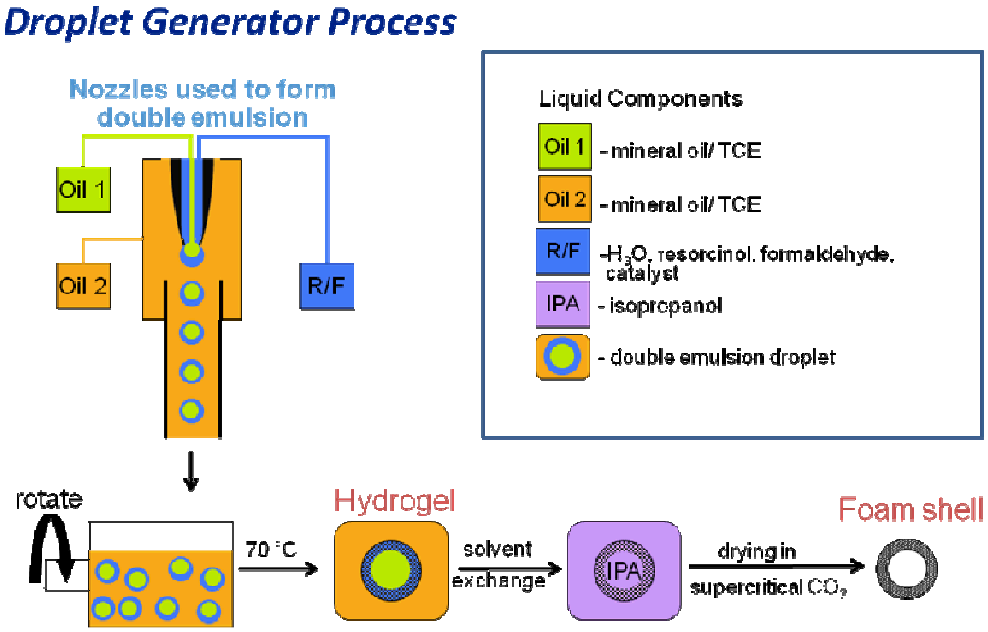

Figure 3.3.1-1 *The Droplet Generator used in the microencapsulation of shell. The specific case is shown for the fabrication of resorcinol formaldehyde aerogel (low density plastic) shells. The fabrication of polystyrene, poly-alpha methyl styrene and divinyl benzene are similar except that the shell wall precursor is oil soluble and can be dispensed with water as the inner and outer fluids.*

A two layer capsule is required for the LIFE target. The outer layer is a solid polymer layer with a wall thickness of 200 µm. The inner layer is a low density (≤30 mg/cc) open cell polymer foam layer with a thickness of 250 µm. Since a large hole for the cone is needed in the capsule there is the opportunity to manufacture either layer first. These two strategies for preparing foam shells in capsules can be placed into two different categories: the "inside-out" and "outside in" approaches.

The potential approaches and relevant steps are summarized as follows:

Foam Shell Option I (inside-out)

- Droplet generation using microencapsulation of oil/water/oil or water/oil/water systems
- GDP coat or mold overcoat

Foam Shell Option II (outside-in); two approaches

- Spin coat interior of shell
- Grow foam from interior surface of shell

Foam Shell Option III (inside-out)

- Form foam film on sacrificial substrate
- Vacuum form foam shell
- GDP coat or mold overcoat
- Alternative: Direct molding of foam shell

Foam Shell Option IV (outside-in)

- Produce capsule shell and bore cone insert hole
- Insert inflatable/deflatable spherical mold into shell
- Form foam film in gap between mold and shell

Foam Shell Option I has been discussed above. The other options are described in the following paragraphs.

Foam Shell Option II *(outside-in)*

There are two distinct paths to achieve this particular approach. The first can be described as spin coating the interior of a preformed polymer shell, and is outlined in the following figure (Fig 3.3.1-2).

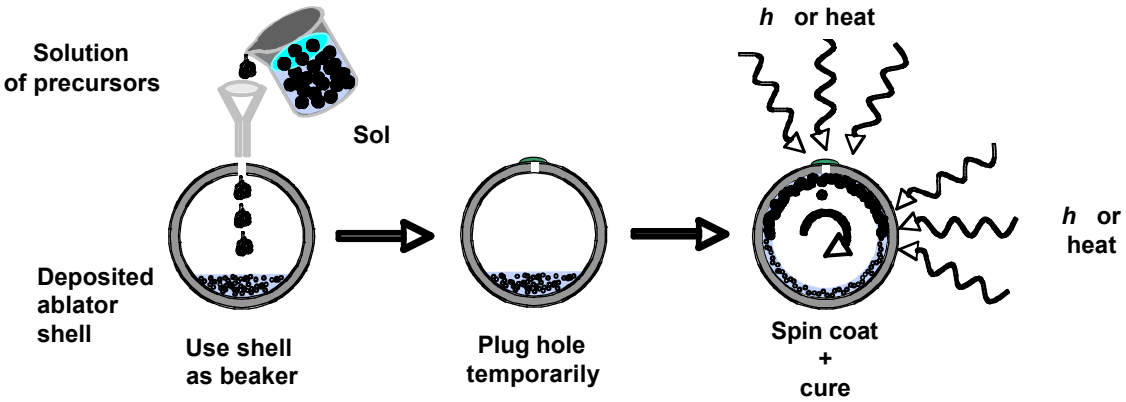

Figure 3.3.1-2 *Process for outside-in approach*

In this approach, a deposited ablator shell is used as the containment vessel for the polymerization reaction. The starting materials are introduced into the shell and the shell

is rotated to uniformly distribute the solution in a "shell" inside the capsule. The final thickness of the fluid layer, and thus the foam, is determined by the initial volume introduced. LLNL has demonstrated the concept by forming a 700-800 um thick DCPD aerogel inside a 1 cm diameter plastic shell. The starting materials were introduced into a hollow plastic sphere that had been attached to a shaft. The assembly was rotated at 3000 rpm (in one direction) and was manually randomly rotated to completely coat the inner surface. Following setting of the gel, the entire assembly was supercritically extracted using CO_2 to produce the final DCPD foam. Challenges that must be addressed include the determination of optimal conditions/technique to provide for a uniform coating to meet the desired concentricity specifications, as well as how to best parallelize such an approach.

The second path would be to initiate the polymer growth directly from interior surface of the capsule shell. This concept is represented in Figure 3.3.1-3 indicating that polymer brushes can be grown from catalytic sites. Polymer brushes are polymers that are attached to a surface at one end with chains that stretch away from the surface. The advantage of this method is that there is no need to introduce a precise volume of reaction mixture into a shell, as well as being able to avoid potentially complex rotational schemes. The ultimate thickness of the foam shell is dictated by the *concentration* of the initial solution. Although a fair amount of research is available on growing full density polymer brushes from surfaces, we need to determine the feasibility of growing cross-linkable polymer brushes from surfaces to prepare porous foams. We have already demonstrated, on a macroscopic scale, that low-density nanoporous hydrocarbon foams are readily prepared using Grubbs' catalysts, a ruthenium based ring opening metathesis polymerization (ROMP) platform. Also, the Grubbs' platform has been shown to be an efficient system for surface initiated polymerization. The Grubbs' catalyst is robust, tolerant of a variety of chemical functional groups, and highly active. This is of particular importance since it gives us freedom in choosing polymer building blocks and architectures to tailor the material to meet a particular need or application. LLNL is currently preparing low-density monoliths with commercially available monomer building blocks. This will allow us to survey potential polymer candidates and to gain valuable insight into designing future polymer systems. Although we have focused on polymers prepared from commercially available dicyclopentadiene and norbornene starting materials, we are also leveraging our synthetic expertise to specifically design polymers using custom prepared monomer building blocks. The custom-prepared building blocks will help optimize polymer chain growth and crosslinking between polymer chains. In conjunction with efforts to grow novel polymeric foams from surfaces we need to define the limits of film thickness growth.

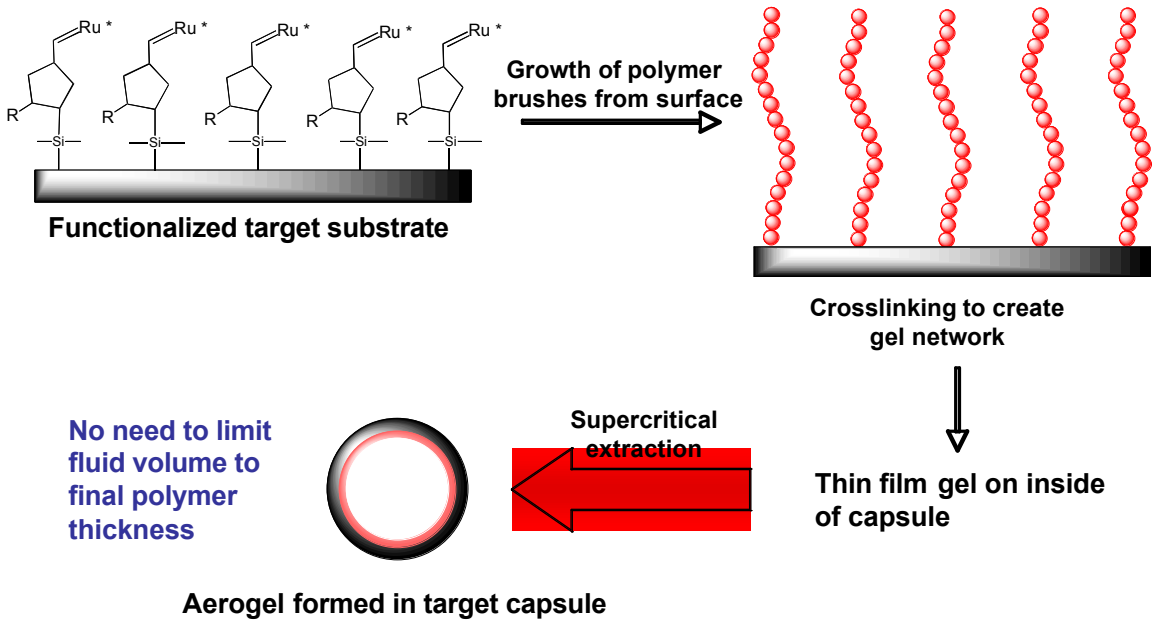

Figure 3.3.1-3 *Second process for outside-in*

Foam Shell Option III (inside-out)

The concept for this approach is to produce a gel film on a thin, flexible sacrificial substrate. The gel thickness should be such that after processing, the resulting foam film will be 250 $\pm$ 20 um thick. The sacrificial substrate likely needs to be stable during the processing including CO_2 extraction. The foam film would be vacuum formed onto a sacrificial mandrel that consists of a spherical portion with a conical section fitting into the sphere (similar to the final foam shape). A polymer coating is then applied to the foam-mandrel ssembly to form the outer ablator shell. It is envisioned that the mandrel be a part of an array of identical mandrels such that a large number foam shells are produced in a single batch. The sacrificial mandrel is subsequently removed using heat or chemical means. Alternatively, an inflatable spherical surface can be used as a mandrel that is subsequently withdrawn from the shell/foam piece following the molding operation.

An issue with this technique is the possible deformation of the initially flat film as it is formed over the spherical mandrel and its effect on the uniformity of the film. It may be necessary to introduce some curvature into the initial film to avoid thinning or wrinkling of the film as it is molded over the mandrel.

Foam Shell Option IV (outside-in)

In this approach the concept is to produce a hollow capsule shell then bore an appropriate cone insert-hole into the hollow shell. An inflatable/deflatable spherical mold/mandrel

would be inserted into the hollow shell and inflated to provide a 250 $\pm$ 20 um gap between the outer surface of the inflatable sphere and the inner surface of the shell. The reactants would be injected into the space between the mandrel and the shell and processed to form a foam film within this gap. Subsequent deflation and removal of the inner spherical mandrel completes the process. Again, it is envisioned that the mandrel be a part of an array of identical mandrels such that a large number foam shells are produce in a single batch. This approach requires a foam formulation that undergoes little or no dimensional changes in the foam during processing. The current formulation for DCPD foams at 30 mg/cc exhibits <5% dimensional change from gel to dried foam. This concept is illustrated in Figure 3.0-2.

3.3.2 Material Considerations

Capsules similar to the LIFE target but without the foam layer have been made at General Atomics for some time as National Ignition Campaign (NIC) indirect drive capsules. These capsules are currently being made to the demanding specifications required for LIFE targets listed above. The NIC shells are fabricated as a coating of glow discharge plasma (GDP) with some dopants such as Ge added for physics needs of the experiment. Because the plastic poly-alpha methyl styrene (PAMS) mandrel is pyrolized away at the end of fabrication the resulting shell is entirely composed of GDP (and whatever dopants were intentionally added). Scaling this process up from the current conditions would be prohibitively expensive due to the long coating times required and the extensive culling of the plastic (PAMS) mandrels used.

Because of the time and cost, it would be advantageous to microencapsulate the whole layer. Since removal of the layer is not necessary, polystyrene(PS) could be used for the whole capsule wall and could take the place of PAMS. A possible issue is whether or not the wall uniformity could be improved to meet the specification. In that case we plan on maximizing the thickness of the PS layer (while not exceeding the NC spec) and coating the remaining layer with GDP.

For foam shells there are a variety of different materials that could be used. None of these foams, however, have yet been made into shells meeting all of the specifications. A variety of materials can be used in the microencapsulation but the most promising are resorcinol formaldehyde (RF) and divinyl benzene (DVB).

At LLNL, a different classes of polymer/catalyst systems are being investigated for use in foam shells. This includes the use of ring opening metathesis polymerization (ROM techniques using, for example dicyclopentadiene (DCPD), is described. ROMP catalysis systems do not require external heating or irradiation to induce polymerization. Even though there has been work showing that DCPD gels can be produced rapidly ($\leq$ 1 hr.) and can be converted to $\leq$30 mg/cc dried foams, there has not been a target shell demonstrated at this density.

3.3.3 Current state of the art

Currently, solid spherical shells made for the NIC meet the specifications, except that the OD variation is higher than specified for LIFE. Currently, for thin (~15um wall thickness) microencapsulated shells the diameter variation is +/- 20 microns at one standard deviation. Other specifications can easily met. The out of round (radius) is 0.5-1 microns for one standard deviation for 2 mm diameter capsules, the wall variation (for thin shells) is <1% avg. NC and the surface roughness meets or is under the NIF spec (20 nm rms).

There is less experience for thick (200um wall thickness) microencapsulated shells than for thin walls. Some thick shells have been made and we are in the process of characterizing those batches. For these shells, there a two major challenges:, wall uniformity and vacuoles.

3.3.4 Throughput and Costs

Table 3.3.4-1. *Estimated cost of proposed capsule fabrication processes (see Appendix A for costing methodology)*

Case	Reject Rate (% Rejected)	Total Capital Cost ($)	Labor ($/yr)	Cost (¢/capsule)
Thick PS	50	$6,145,120	$2,106,000	1.2
Thin PS, GDP-coating	5	$152,142,487	$3,306,000	5.2
DVB foam, GDP coating	50	$221,981,113	$3,906,000	7.8
Injection molded capsule	5	$28,775,590	$3,831,000	1.6

3.3.5 Research Needs

Because of the tight capsule specifications, it is likely that some fraction of the micro-encapsulated capsules will not be of sufficient quality for injection into the target chamber. It is therefore necessary to institute an inspection process to measure every shell and to reject non-conformal shells. It is important that this measurement happens early in the fabrication process before additional value is added to the capsule assembly. A challenge for this inspection process, however, will be 100% inspection of all targets at the production speed. To accomplish this, we will develop an automated optical inspection system. This automated system will measure the diameter, wall thickness, and wall thickness uniformity of each shell at a speed sufficient so that a small number of

these systems could measure and reject shells in real-time for a commercial power plant design.

For solid shells, a number of research topics can be pursued to address the high cost of producing thick capsule shells. Micro-encapsulated thick-walled shells will cost much less than vapor–phase deposited GDP shells. Even assuming a high reject rate of shells from the microencapsulation process it would still be several times cheaper per shell (Table 3-3). The first step will be to optimize the encapsulation process parameters. This will include optimization of the concentration and molecular weight of the polystyrene which influence the viscosity of the compound droplet wall. We will then make a variety of wall thicknesses under various conditions and determine the maximum thickness that could be made without exceeding the wall uniformity specification. We will use dielectrophoresis (DEP) forces generated by electric fields to further improve the wall uniformity by using DEP to force the inner droplet to align with the shell droplet. There is an ongoing collaboration between U of Rochester and General Atomics to work on this, and we believe that this will be ready as early as FY2011. This subject of this effort is to find a compatible fluid system for DEP (low conductivity, immiscibility, proper dielectric behavior, etc.) and the optimal electric parameters (voltage, frequency, voltage envelope, electrode configuration) to achieve a uniform wall.

We will also optimize the geometry of the encapsulation chamber and the dispensing needles and implement a feedback loop to decrease the variability of the capsule diameters.

For foam shells with a solid GDP overcoat, we will work on optimizing the foam material and reducing the cost of the overcoat. We will begin by investigating several foam systems to find one with the best properties and mechanical strength at the required density. Many foam materials lose significant strength at low densities so finding a foam material that is both low density and able to withstand the forces of manufacture and injection into the target chamber is imperative. We will then work to optimize the GDP coating parameters for fast coating rate and smooth surface, two competing specifications. The outside-in scheme, Option II, will be pursued in parallel with Gen I microencapsulation and ROMP systems. Alternate schemes, Options III and IV, will be investigated later if progress in the initial schemes is slow or unpromising.

3.3.5-1 Research timeline

	FY 09	FY 10	FY 11	FY 12	FY 13	FTE years
1. Inspection & culling system						
Proof of principle device testing	←	→				1
Rep rate scale up		←	→			2
2. Solid shells						
Optimize thick wall microencapsulation for NC	←	→				1.5
Shell dimensions (optimize precision of droplet dispensing)		←	→			1.5
DEP to center shell		←	→			1
Coatings (increase coating rate while minimizing roughness)		←	→			1
Rep rated hole cutting			←	→		1
3. Foam shells						
Encapsulation at required density	←	→				1.5
Improve sphericity and yield		←	→			1.5
Coatings on foam			←	→		1
ROMP shell encapsulation	←	→				0.5
Improve ROMP shell sphericity and yield		←	→			0.5
Option II (outside in)	←	→				
Improve Option II wall uniformity and yield			←	→		1
Option III (mold on sacrificial mandrel)		←	→			1
Option IV (mold on deflatable mandrel)		←	→			1
4. **Process Scale Up testing**				←	→	6
5. Plant conceptual design					← →	2

Total: 25 FTE years over 5 years
Other costs: $2 million in equipment and ODC

3.3.5-2 Summary Chart

Case	Figure of merit	Cost (¢/ea)	Throughput	Current Specs	Risks	Probability of Success
Thick PAMS	Wall uniformity (NC), sphericity, areal density uniformity, surface roughness	1.2	6DG at 4Hz, 7 day process time	NC<1%, OOR <0.1%, Density non-uniformity<10%	NC, OOR, vacuoles (voids in shell wall)	High
Thin PAMS, GDP-coating		5.2	6DG at 4Hz, 45 day process time (dependant on coating rate and thickness)		Cost (slow coating rate)	High
DVB foam, GDP coating		7.8	6DG at 4Hz, 51 day process time (dependant on coating rate)		Fragility of foam layer, surface roughness of capsule	Medium
Injection molded capsule		1.6				

3.4 Diamond ablator shells

Besides beryllium and plastic, diamond is one of the ablator materials which is currently being evaluated for the ICF application. Diamond has a unique combination of physical properties which makes it a very promising ablator material. Specifically, diamond's extremely high atomic density guarantees efficient energy adsorption (better than plastic and beryllium), and its extremely high yield strength may be utilized to suppresses the development of instabilities at the ablator/fuel interface. Furthermore, diamond is chemically extremely inert, which allows one to apply very aggressive processing and cleaning procedures; finally, synthetic diamond is an environmentally friendly material that, despite of diamond's reputation as an expensive material, can be produced cost-efficiently. Actually, the main ingredient necessary to synthesize synthetic diamond by chemical vapor deposition (CVD) is methane, and the material costs are only in the order of a few cents per target.

3.4.1 Description of the diamond CVD process

In a joint research project, LLNL and the Fraunhofer Institute for Applied Solid State Physics in Freiburg, Germany succeeded in developing an environmentally safe and cost-efficient batch process that allows one to produce large quantities of ultra-high precision diamond shells for the NIF ICF application.[1] The fabrication of diamond capsules is a multi-step process which involves diamond chemical vapor deposition on silicon mandrels followed by polishing, microfabrication of holes using a laser, and removing of the silicon mandrel by an etch process (see Figure 3.4.1-1).

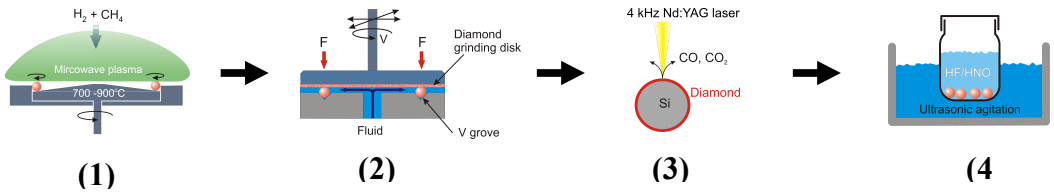

Figure 3.4.1-1 *Fabrication of diamond capsules is a multi-step process which involves the following steps:1) microwave assisted chemical vapor deposition, 2) ultra-high precision polishing, 3) Nd:YAG laser hole machining, and 4) ultrasonically assisted wet etch.*

The key technology is the coating of the spherical Si mandrel with a uniform, void-free, approximately 100-µm-thick diamond film using a microwave plasma-assisted chemical vapor deposition (PACVD) process. To achieve a uniform coating, the Si mandrel is continuously rotated during the PACVD process by using a rotating sample platform capable of holding large batches of the mandrels. At a deposition rate of 2 µm/h, it takes approximately 50 hours to deposit the required film thickness of 100 µm using a feed gas mixture of 1% methane in hydrogen at a deposition temperature of 700-900 ^{o}C. For the ablator application, nanocrystalline diamond (NCD) is preferred over coarse-grained material as its isotropic character reduces the risks associated with the crystalline nature of diamond in the context of shock physics. As previously demonstrated by LLNL, thick

and void-free NCD films can be grown by controlling the secondary nucleation rate by adding ppm levels of oxygen and/or nitrogen to the CH_4/H_2 gas phase chemistry.

3.4.2 Current state of the art

Using this process, diamond shells which meet all the stringent requirements of the NIF ICF application have successfully been made. However, for the LIFE application, the production costs must be lowered considerably. Currently, the most cost-intensive process step of the fabrication of diamond shells is the diamond CVD process. Without changing the current technology, the diamond deposition costs can be lowered by running larger batches. The effect of this scaling-up on production costs is illustrated in table 3.4.2-1.

Table 3.4.2-1: *State-of-the-art diamond ablator technology and costs*

Diamond CVD			
Assumptions	2 mm mandrel / 100 micron thickness (~10^{-3} cm^3 diamond => 3.5 mg => $3x10^{-4}$ mol/shell)		
Number of shells/batch		50 (current technology)	750 (upper end of current technology)
Chemical energy	CH_4 => C+ H_2 ΔH = 74 kJ/mol	0.02 kJ/shell or ~ $6x10^{-6}$ kWh/shell or ~10^{-4} cts/shell	
Electricity	500 kWh @ 12 cts/kWh (10 kW x 50 h) => $60/batch	120 cts/shell	16 cts/shell
Materials	Gas mixture CH4: ~$150/$m^3$, H2: ~$2.5/m^3 CH_4 : H_2 = 1:99 ~$4/$m^3$ Gas consumption ~ 1 m^3/h	8 cts/shell	0.5 cts/shell
	Theoretical limit (no waste) $CH_4 + 2H_2$ => C + $4H_2$ 3.5 mg diamond/shell => $3x10^{-4}$ mol CH_4/shell or 0.12 cts => $6x10^{-4}$ mol H_2/shell or 0.004 cts	0.125 cts/shell	
Capital equipment	50 h/batch => 175 batches/Y Reactor cost $300k Depreciation 7Y/linear	~$5/shell	32 cts/shell
Total costs/shell	Not including etching and polishing	~$6/shell	~50 cts/shell

Hole machining and etching are relatively inexpensive and can be neglected in a first order estimate of the costs. The cost of polishing, on the other hand, depends strongly on the required surface finish. Consequently, this step can be very expensive for NIF ICF targets, but may be inexpensive, or not necessary at all, in the case of LIFE targets which are more forgiving concerning surface roughness (peak-to-valley roughness ~ 1 micron

rather than 100 nm for NIF ICF capsules). Beyond scaling-up, the production costs could be further lowered by increasing the deposition rate (a factor of two is reasonable) and developing lower-cost or larger batch reactor designs (again a factor of two is reasonable). Together, these improvements could lower the costs per shell by a factor of four, that is, from 50 cts per shell to ~12 cts per shell. Also, the availability of cheaper electricity would lower the costs considerably (the cost calculation in table 3.4.2-1 is based on standard household rates). The cost of the silicon mandrel needs to be added to the tabulated cost.

3.4.3 Research Needs

In the case of diamond ablator shells, the research will be focused on reducing the costs rather than improving the quality which is already more than sufficient. Specifically, the following research areas need to be addressed:

1) Demonstration that scaling-up of the current technology can be done with out jeopardizing the quality of the diamond shells
2) Increasing the deposition rate by a factor of two without degrading the material quality
3) Developing more efficient, high throughput seeding techniques while maintaining the high nucleation density currently achieved (e.g. using colloidal solutions of diamond nanoparticles)
4) The development of thick ultra-smooth NCD films to avoid polishing (RMS surface roughness less than 100 nm)
5) Exploration of the potential benefits of the hot-filament CVD (HFCVD) diamond process (thick ultra-smooth NCD, larger deposition area, larger batches)

Specifically, the development of thick ultra-smooth (mirror finish) NCD films needs to be pushed forward to avoid polishing. The deposition of smooth, thick NCD films on planar substrates via hot-filament CVD (currently PACVD is used in the fabrication of diamond ablator shells) has already been demonstrated[2]. In a second step, this technique needs to be transferred from planar substrates to spherical substrates.

3.4.4 Research timeline and costs

Table 3.4.4-1 *Proposed research timeline and costs associated with development of diamond ablator capsules*

	FY 09	FY 10	FY 11	FY 12	FY 13
scaling-up / current technology	←	→			
Increasing the deposition rate	←	→			
Developing new large scale seeding techniques		←	→		
thick ultra smooth NCD	←	—	→		
Exploring the HFCVD process		←	—	→	
Demonstration of a 10cts/shell feasibility				←	→
Costs	$600k	$800k	$800k	$1000k	$1000k

3.3.5 Conclusion

In conclusion, the fabrication of ultrahigh precision diamond shells has already been demonstrated. Lowering of the production costs could be achieved by a combination of scaling up the current technology, and using higher deposition rates as well as lower-cost deposition equipment. The development of more efficient high throughput seeding techniques and of ultra-smooth NCD films on spherical substrates will be required. Finally, the hot-filament CVD diamond process has the potential to further lower the production cost by running much larger batches.

References:

1. Biener, J.; Mirkarimi, P. B.; Tringe, J. W.; Baker, S. L.; Wang, Y. M.; Kucheyev, S. O.; Teslich, N. E.; Wu, K. J.; Hamza, A. V.; Wild, C.; Woerner, E.; Koid, P.; Bruehne, K.; Fecht, H.-J. *Fusion Science & Technology* **2005,** submitted.
2. Kucheyev, S. O.; Biener, J.; Tringe, J. W.; Wang, Y. M.; Mirkarimi, P. B.; van Burren, T.; Baker, S. L.; Hamza, A. V.; Bruehne, K.; Fecht, H.-J. *Applied Physics Letters* **2005,** 86, 221914.

3.5 DT Layering

3.5.1 Description and specifications

A layer of the deuterium-tritium (DT) fuel, uniform in thickness, covering the inside surface of the ablator capsule is required for ignition. In the ignition designs currently considered for the LIFE Engine, a 250-micron-thick low-density, low-Z (<30 mg/cc) nanofoam is placed inside the ablator (Fig. 3.5.1-1). The purpose of the foam is to wick the DT fuel, maximizing the amount of DT in the layer deposited on the inner wall of the ablator and minimizing the amount of DT deposited on the high-Z cone.

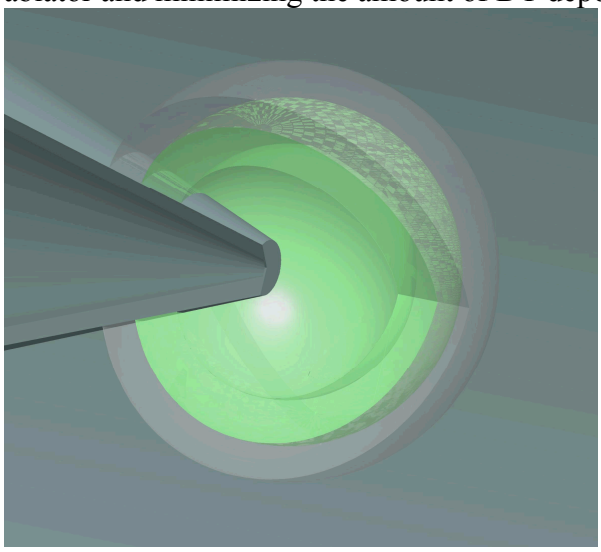

Figure 3.5.1-1 *Schematic showing a fuel capsule and the high-Z cone. The current target design demands that the low-density nanofoam (shown in light-green) wick most of the DT fuel, while the deposition of the DT ice on the high-Z cone be minimal.*

Table 3.5.1-*1 lists the current specifications relevant for DT layering processes.*

Item	**Specification**
Initial DT temperature (K)	(~10-16 K) TBD
Stresses during target handling and injection (MPa)	TBD
Ablator inside diameter (mm)	2.00±TBD
Ablator wall thickness (mm)	0.20±TBD
Foam layer thickness (mm)	0.25±TBD
DT layer thickness (mm)	0.25±TBD
Maximum DT/ablator interface roughness	TBD
Maximum DT/vapor interface roughness parameter (micons)	TBD
Maximum concentration of high-Z impurities (at.%)	TBD
Maximum He concentration (at.%)	TBD
Maximum mass fraction of DT deposited on the cone	TBD

From the viewpoint of DT layering, the major differences between such LIFE-engine targets and the hot-spot ignition targets currently extensively studied for the National Ignition Campaign (NIC) include (i) a much thicker DT layer; (ii) the presence of a metal cone breaking spherical symmetry, (iii) a nanofoam, potentially affecting hydrogen crystallization and evolution on cooling; and (iv) a much lower temperature of DT (~10-16 K for LIFE, compared to ~18 K for NIC), inherent to fast ignition designs, requiring a lower initial DT vapor pressure inside the capsule.

3.5.2 Processes

Filling

Several approaches for capsule filling have to be evaluated. Capsules could be permeation filled with DT by placing the capsules in a chamber where the DT pressure is increased to the values needed for filling capsules with the required number of hydrogen molecules. This assumes that the capsule material exhibits similar permeation rates for all the three molecules of the fuel gas mixture: D_2, T_2, and DT. The permeation process has an advantage over the other processes currently considered for capsule filling, such as fill-tube and fill-hole assisted filling, because it affords for parallel filling of a large number of capsules. Such a parallel processing is essential for the requirement of making ~10 targets per second. Several technologies for parallel filling of targets have previously been discussed in the literature. Disadvantages of permeation filling include safety issues associated with any high pressure process and a large inventory of tritium required. Therefore, the alternative approaches for DT filling mentioned above should also be considered.

Cryogenic Layering

Cryogenic layering refers to the process of redistribution of DT fuel on the inside wall of the capsule. Since DT has a very high equilibrium vapor pressure at the melting point, LIFE target designs call for initial fuel temperatures lower than those for central hot-spot ignition targets. Hence, cryogenic layering will involve solid rather than liquid hydrogen A major technological goal is to identify optimum process parameters (in particular, temperature-time profiles) resulting in sufficiently smooth DT layers.

Even if before solidification all the liquid DT is wicked inside the nanofoam, making a uniform in thickness solid DT layer inside the ablator capsule could be a challenge since it involves an inherently unstable rapid crystallization on undercooling in the presence of thermal gradients. Indeed, the solidification process could dramatically change DT thickness uniformity. Additional challenges include achieving a sufficiently smooth DT solid/vapor interface and keeping the metal cone with a minimal amount of hydrogen deposited. On cooling, DT melt crystallizes to the hexagonal closed packed (hcp) structure. A radial thermal gradient caused by beta-layering is expected to aid the formation of smooth DT layers. However, the processes of DT crystallization and structure evolution on cooling are complex, and non-trivial topography of the DT/vapor

interface typically develops. Since not much is currently known about the formation of thick DT layers inside nanoporous scaffoldings, research will need to be done to optimize the layering process. Achieving spherical isotherms in the presence of the symmetry breaking metal cone is another challenge.

3.5.3 Research Needs

The LIFE target design puts unprecedented requirements on DT layering. Current NIC target designs call for <100-micron-thick DT layers in 1-mm-diameter capsules held at ~18 K. Best quality layers are single crystal hcp DT grown from a melt in a setup with a fill tube, in an integrating sphere, with typical growth times of >10 h. If polycrystalline DT layers with the DT/vapor interface decorated with ~10-um-deep and ~20-um-wide grooves are acceptable for LIFE targets, a list of challenges to be addressed include engineering spherically isothermal conditions around each shell in a massively parallel process, understanding DT growth inside nanoporous scaffolds, suppressing DT growth on the cone, and controlling the formation of He bubbles due to tritium decay. For more stringent groove density requirements, none of the current mass-production approaches could be directly applied. An aggressive materials research program is needed before any significant engineering efforts. This is a complex materials science problem, involving crystal growth and mechanical deformation of a quantum alloy, when a close interaction between experiments, theory, and modeling is essential for success.

The initial general research needs could be summarized as follows:

- Clarification of target design specifications (in particular, shot temperature and DT ice roughness).
- Understanding behavior and mechanisms of DT crystallization inside nanoporous scaffolds. Will the DT layer grow as a single crystal hcp or as a polycrystal with heavily grooved surface? Could smooth nanocrystalline or amorphous layers be grown in scaffolds?
- Achieving templated DT growth so that the metal cone has a minimum amount of DT deposited.
- Understanding mechanisms of DT evolution during cooling. Can we control grain boundary growth by a delicate choice of the temperature-time profiles? Could we improve relevant properties of DT ice by doping?
- Based on results of the behavior of DT wicked inside nanoporous solids, alternative approaches for DT filling should be considered.

3.6 Assembly

3.6.1 Description and specifications

Assembly operations are required when two or more sub-components must be aligned and bonded during the automated fabrication of the target. In the current process plan, assembly processes are required to:

- Join parts of the hohlraum if molded in multiple segments
- Join parts of the hohlraum and cone if they are not manufactured in an integral fashion
- Join two halves of the capsule if required
- Laser drill a hole in the capsule for foam fill if needed
- Align and glue the cone to the capsule (See Figure 3.6.1-1)

The alignment and bond specifications for these assembly operations are listed in the table below (*No official specifications are available at this time*):

Process	Alignment tol.	Joint mat'ls	Bond specs.
Join hohlraum parts	< 10 um	Glue, solder, weld	
Join cone-hohlraum	< 10 um	Glue, solder, weld	
Join capsule halves	< 2 um	Glue, solder, weld	
Drill hole in capsule	< 5 um	laser	
Join capsule - cone	<5 um? Maybe ~2 um	glues	Glue can penetrate foam < 60 um ; glue volume ~10 nl

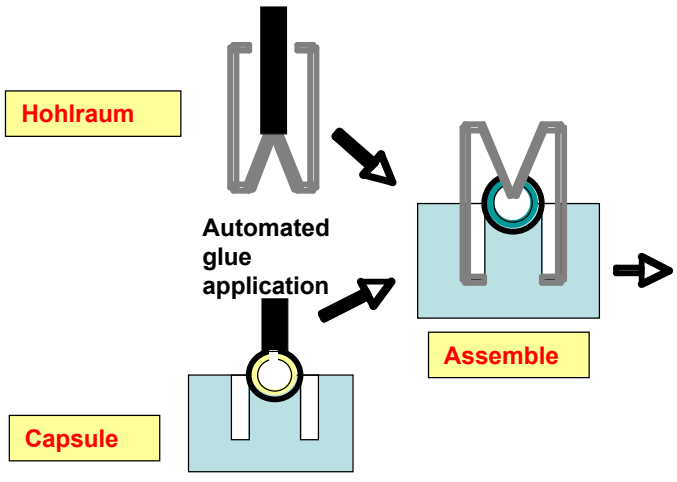

Figure 3.6.1-1 *Pictorial of assembly and glue operation of cone to capsule*

3.6.2 Material Considerations

Materials to be joined are expected to be lead for the hohlraum and polymers of some variety for the capsule and foam components. The capsule could also consist of a low Z material such as beryllium or diamond. Joint materials are most likely to be polymeric glues although metallic bonding procedures such as welding or soldering could be used for metallic parts. US patent 3772750 recommends an electron beam weld joint to mate two halves of hollow ball bearings. World intellectual property organization document WO 2008002508 20080103 suggests that laser welds are a better technique for joining hollow ball bearing hemispheres. Regardless of the joint material and method, care must be taken to ensure that excess material is minimized and that all voids, pits and scratches are filled.

Glues must be able to survive and maintain leak-tight seals at cryogenic temperatures down to 15 K. Glue joints should be thin to avoid spatial variations in geometry and material composition. Glue viscosities are important to the dispensing process.

3.6.3 Processes

3.6.3.1 Assembly and glue

Fixturing

Automated assembly can be accomplished using either hard or flexible tooling. Hard tooling implies building custom assembly machines designed specifically for the process being performed and for the specific parts begin manipulated. Many high-throughput factories such as candy manufacturing use this type of custom-designed tooling. Flexible tooling, including robotics, is used where operations are changeable or intricate, requiring motions not conducive to fixed tooling. In general, fixed tooling can be a faster, cheaper method of manufacture. At throughputs of roughly 1.7 M /day for >20 years for target fabrication, fixed tooling investments are expected to be recouped. Use of off-the-shelf pick-and-place type mini-robots combined with custom fixturing represents a hybrid between fixed and flexible tooling

Typical fixed/semi-flexible tooling for glue assembly might look like that shown in Figure 3.6.3.1-1. One of the two parts rests in a fixture specifically designed to locate the parts being assembled. These parts can be arrayed such that operations can be performed on multiple parts simultaneously. A glue dispenser or stamp can apply glue only where needed. The second part can be mated with the first part using a pick-and-place mini-robot such as the one shown in Figure 3.6.3.1-2 with the alignment guaranteed by the matchup between the fixture for part-one and the compliant end-effector/fixture for part-two. The alignment tolerance for such a mating scheme is depends on the tolerance of the part, the fixture part holder/locator, and the fixture alignment mechanism. Typical fixture alignment accuracies are on the order of 1 to 5 um. The throughput for

one operation is expected to be on the order of 1 operation per 0.5 to 3 seconds. Individual tooling costs can range from $5,000 to $30,000.

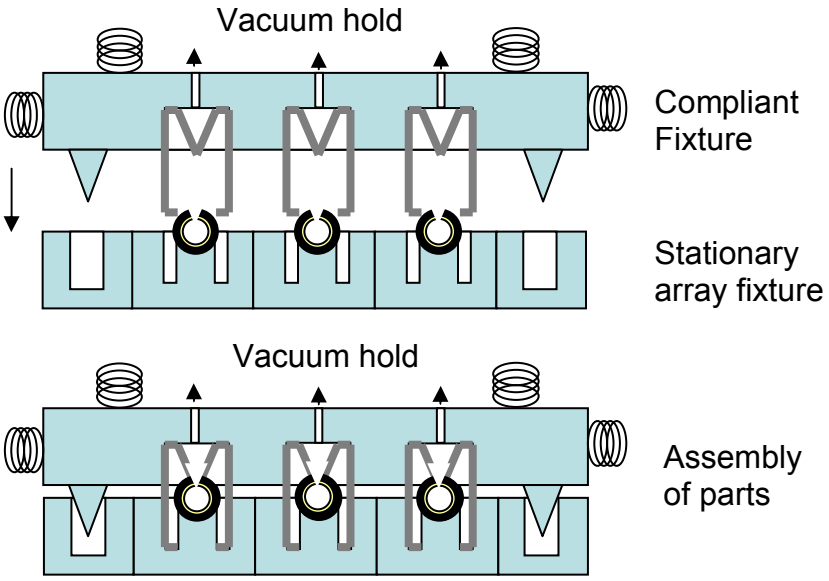

Figure 3.6.3.1-1 *Fixture for array assembly of cone to capsule*

Figure 3.6.3.1-2 *Small SCARA robot for pick-and-place*[1]

An example of a fully flexible assembly scheme is shown in Figure 3.6.3.1-3 for attaching two parts. In this example, a 6-axis robot locates the first part using a vision system. The robot applies glue though a glue dispensing system in a pattern programmed into the robot. The robot picks up part-two using the vision system and aligns and glues the two parts together. The alignment accuracy for a system such as this can be about 15 um (Adept robots). Alignment fiducials imprinted on the part can aid in the visual alignment of parts. The throughput for one operation is expected to be on the order of one operation is 3 sec. Tooling costs can range from $20,000 to $50,000.

Figure 3.6.3.1-3 *Six-axis assembly robots on the plant floor*

Higher assembly precision could be achieved through of ultra-precision linear motors such as those supplied by Aerotech which can have accuracies of 0.2 um over 500 mm (Model ABL 1500). Final placement of parts using such an actuator can provide the required alignment tolerance. Multiple units of small, custom-built systems with precision X-Y placement may be an acceptable solution if the units are less than about $5000 each. In this case, 60 units at a total price of $300,000 can provide the required throughput.

Self-fixturing techniques such as the one suggested in Figure 3.6.3.1-4 below can be used to provide alignment accuracy at low cost and high throughput. In the suggested configuration, the cone can be a separate component and subsequently attached to the hohlraum. The cone can fit into a mating feature on the hohlraum for a self-fixtured alignment. A flange is added to a non-critical side of the cone to mate with the capsule in such a way as to locate the part without external fixturing. Another solution to hohlraum assembly could be the use of snap-together features to eliminate the glue operation entirely which reduces the time and complexity of the assembly task.

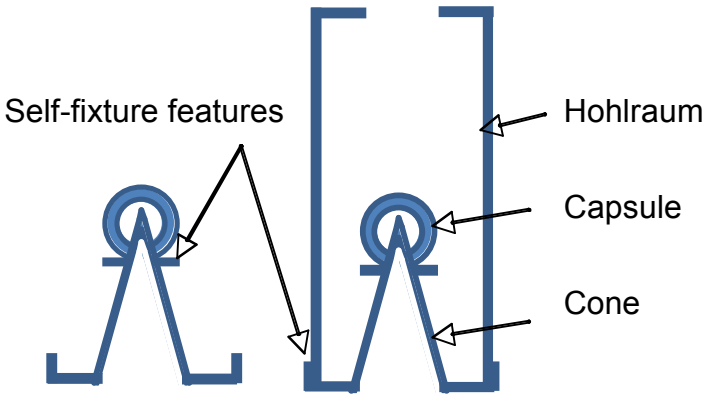

Figure 3.6.3.1-*4 Self-fixtured assembly*

Gluing

Glues such as those from Dymax are currently being used to glue components for NIC targets. These glues must form leak-tight seals at temperatures down to 15 K. Current glue dispensers being used for NIC dispense in volumes of 10s of nL. Ink-jet printers are able to dispense in volumes of 50 to 500 pL. The smallest gap currently filled in the NIC target is the 2.5 pL gap between the capsule and the filltube. Filing this gap precisely is a very difficult task involving the wicking of material into the gap during contact with a pre-filled capillary tube. The timing, gap geometry and shear dependant viscosity properties of the glue are all important parameters in making this joint. The glues are all UV cure glues to reduce the polymerization time and to better control the timing of the glue operation. Polymerization time must be added to the alignment time for the total assembly and glue operation time. Typical polymerization times for UV glues are about 2 minutes.

Throughputs and Costs

Throughput and costs are summarized in the Table below:

Process	Accuracy	Time per operation	Number per operation	Time per target	Capital cost	Cost per target
Fixed tooling-glue	50-500 pL	~5 sec	60	.08 sec	$50,000	Neg.
Flexible tooling	~2 um	~3 sec	60	.05 sec	$60,000	Neg.

Research needs

Principle research needs include the ability to handle delicate parts and to locate them accurately in a fixture. Location accuracies will result from dimensional tolerances of the part, the fixture and any allowance required for sliding fits if needed. Research needs for fixturing include:

- Design and build high accuracy, compliant fixturing to reduce part location accuracies to < 1 um and fixture alignment accuracies to < 1 um
- Determine techniques to mate "upside down" hohlraum to capsule (or visa-versa) through vacuum hold or other techniques

Automatic part bonding methods must be investigated. The details of glue joints can involve a significant amount of study if they are to be made in a fashion which minimizes the time of the glue operation and minimizes the amount of glue which migrates away from the bond area. Glue dispensing accuracies of 100 pL is desirable to make accurate glue lines of 10 nL. This is the limit of the dispensing capabilities of current ink-jet

printers. Mechanisms for precise glue dispensing or glue stamping must be considered. Wetting properties of the glue to the parts must also be studied. Ideally, the glue covalently bonds to the underlying material and does not wick or spread outside the bond area. The current NIC target bonds are at about one third the covalent bond strength (Suhas Bhandarkar). Research topics for the glue joint include:

- Select or develop cyrogenic glues for ability to perform as required
- Develop picoliter dispenser for glue (~100 pL)
- Develop method for application around part in single application
    - Nozzle for simultaneous dispensing around a circle
    - Pin application around perimeter
    - Glue stamp process
    - Groove around cone to wick glue creating an even distribution
- Prevent migration of glue
    - Study the surface energy modifications of glue and substrate
    - Tune viscosity and polymerization time of glue
- Minimize polymerization time to reduce operation cycle time
- Investigate alternative bonding methods
    - Laser welding of hohlraum parts
    - Solder of hohlraum parts

Assembly Development Plan

	FY 09	FY 10	FY 11	FY 12	FY 13
Develop hohlraum/cone assy				←	→
Develop capsule assy				←	→
Develop cone-capsule assy			←		→

3.6.3.2 Automated Handling in Production Line

Description and specifications

The entire target fabrication line must be fully automated in order to meet the throughput and cost objectives for the targets. A possible exception to this rule is loading and unloading bulk quantities of target parts from a large batch processes. This will necessitate the development of fixtures and machinery to move the targets seamlessly from one process to the other. Conveyor systems, vibratory hoppers and pick-and-place devices are typical meads of transporting parts from one fabrication station to the next. It is most likely that we will outsource the design of the transport system to an automation house such as E and M of San Francisco.

Research needs

Automated factories are commonplace. Consumer-product-based factories produce thousands of a particular product very cost-effectively. Many standard techniques can be applied to the target fabrication factory. An area of research might be special handing for very fragile parts, depending on the final target design.

References:

1. http://www.adept.com/

3.7 Emerging Fabrication Technologies

There are several emerging micro- and nano-fabrication technologies which may significantly contribute to LIFE target fabrication. They may have impact on all major fabrication challenges including hohlraums, capsules, and foam geometries. These technologies, Projection Microstereolithography, Electrophoretic Depsotion, and the Hollow Jet Instability Method discussed in the following sections.

3.7.1 Projection Microstereolithography

Process description

Baseline concept

Projection Microstereolithography (PμSL) with a Digital Micromirror Device (DMD) or Liquid Crystal on Silicon (LCoS) display is capable of fabricating complex three-dimensional microstructures in a bottom-up, layer-by-layer fashion. A CAD model is first sliced into a series of closely spaced horizontal planes. These two-dimensional slices are digitized in the form of a bitmap image and transmitted to the DMD (or LCoS). A UV source illuminates the DMD which acts as a dynamically reconfigurable photomask and transmits the image through a reduction lens into a bath of photosensitive resin. The resin that is exposed to the UV light is cured and anchored to a platform and z-axis motion stage. The stage is then lowered a small increment and the next two-dimensional slice is projected onto the resin and cured on top of the previously exposed structure. This continues until the three-dimensional part is complete such as those shown in Figures 3.7.1- 2 and 3.17.1-3.

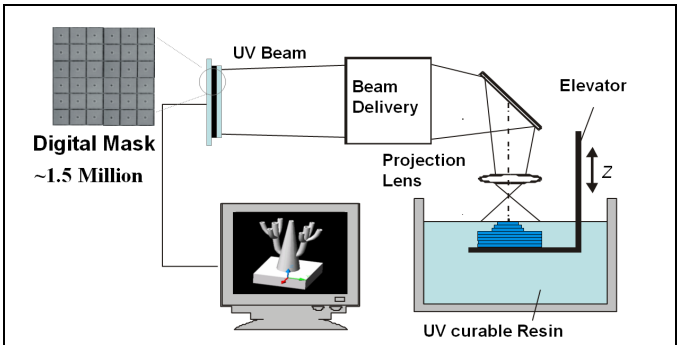

Figure 3.7.1-1 Schematic of baseline PμSL system currently at UIUC [1].

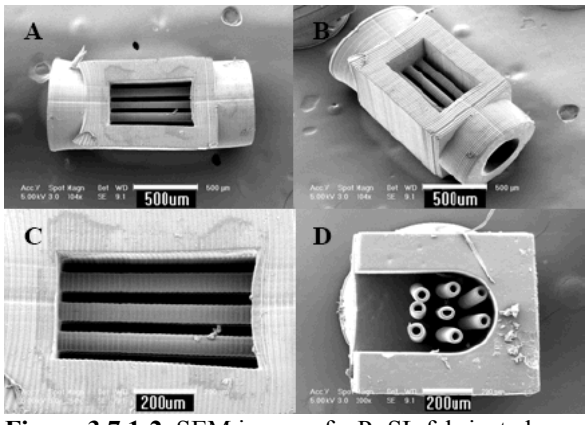

Figure 3.7.1-2 SEM image of a PμSL fabricated bioreactor [1, 2]

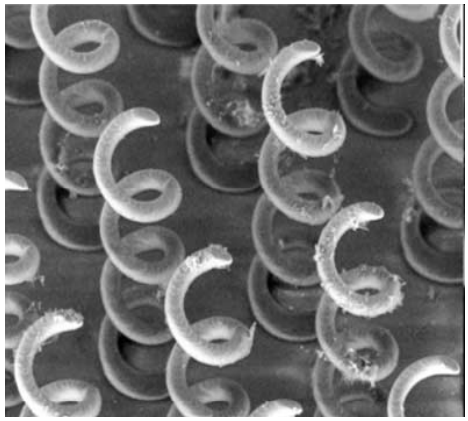

Figure 3.7.1-3 SEM image of PμSL fabricated coils [3].

Nanofabrication with a superlens

Imaging and lithography using conventional optical components is restricted by the diffraction limit. Resolution in these systems is limited to one half of the wavelength of the incident light because they can only transmit the propagating components emanating from the source. Subwavelength information is carried by evanescent waves which decay exponentially in mediums with positive permittivity and permeability. The information contained in these waves is lost long before reaching an image plane.

Recently, work by Pendry[4] has predicted that a so-called "superlens" can amplify the evanescent waves thus restoring the image which exists below the diffraction limit. Typically, this lens takes the form of a thin layer of material with either negative permittivity or permeability (resulting in a negative index of refraction). Noble metals such as silver are good candidate materials due to the ability to generate negative permittivity by the collective excitation of conduction electrons. By designing a thin metal slab such that the surface plasmons match the evanescent waves being imaged, the superlens enhances the amplitude of the field. This enhancement of evanescent waves by surface plasmons in silver films was first reported by Fang (our collaborator) and co-workers [5]. They also showed the first demonstration of a silver film superlens by imaging features onto photoresist[6] at ~1/6λ. A schematic of this superlens is shown in Figure 3.7.1-4.

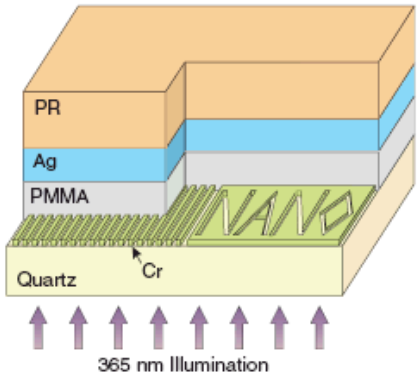

Figure 3.7.1-4 Schematic of thin-film silver superlens [6].

To utilize this near-field effect in a PμSL system, it must be converted to a far-field phenomenon. The amplified evanescent waves can be converted into a propagating field by using thin-film silver grating-type structures[7]. Further development of this far-field concept for integration into a PμSL system will allow for rapid direct writing of three-dimensional nanostructures below the diffraction limit. To date, superlens' have only been utilized for imaging purposes.

Digital holographic nanolithography

Holographic nanolithography has emerged as a method of three-dimensional volumetric nanofabrication. This can also be integrated with the PμSL system for advanced target design. This method can create designed defects and aperiodic

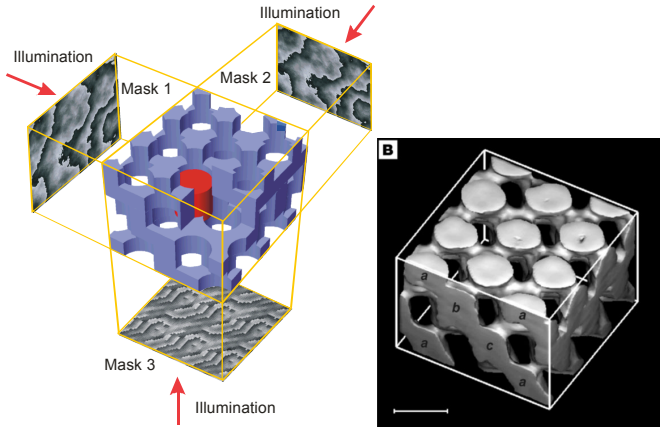

Figure 3.7.1-5 Synthetic holographic nanolithography reproduces complex 3D crystallographic orders in a single snapshot; proof-of-principle demonstration by Campbell *et al* [81]

micro- and nano-structures by interfering light from multiple DMD or LCoS devices in the resin bath. This will allow a variety of porous structures and materials to be fabricated and point features to be intentionally positioned. The digital dynamic masks can be exploited to project a computed three-dimensional hologram into liquid polymers for fabrication of highly interconnected functionally graded density materials with 10s-100s of nanometer precision. It should be possible to achieve meso-scale (>1 mm) components while maintaining quarter-wavelength resolution of 70-100 nm.

Application to target fabrication

PμSL on its own, integrated with a plasmonic superlens, or in a holographic configuration can all make important contributions to target fabrication for LIFE. There are three components to be fabricated:

1. Hohlraums – The baseline PμSL process should be capable of fabricating hohlraum type geometries in polymers or with polymers mixed with metals and ceramic particles. Components with metal or ceramics can be sintered to yield an all metal/ceramic part provided that shrinkage is accounted for. An all polymer hohlraum could be later coated with gold or other metals of interest as well.
2. Capsules – The baseline PμSL process should be able to fabricate shell type structures and with an integrated superlens, nanoscale features and tolerances are possible. Capsules could be made of polymers or ceramics and metals with the use of particles and sintering.
3. Foam structures – There are several methods for generating graded density and foam materials with PμSL. Simply by using the "gray scales" of the DMD or LCoS dynamic mask, some control of porosity can be achieved. The varying light intensity will result in partial polymerization and some local void spaces. With holographic nanolithography, foam structures resulting from interference patterns can be produced with pores sizes in the 100s of nanometers possible.

In addition to fabricating these structures, PμSL is also a highly scalable technology. With larger optics or multiple digital mask devices, PμSL can be expanded for wide area fabrication. This could lead simultaneously batch fabricating thousands to tens-of-thousands of structures. While producing a single part may take many hours, producing thousands over a wide area should not take any longer making the per part production time much smaller. This is similar to the economies-of-scale enjoyed by other batch fabrication processes such as those which enabled the entire microelectronics industry.

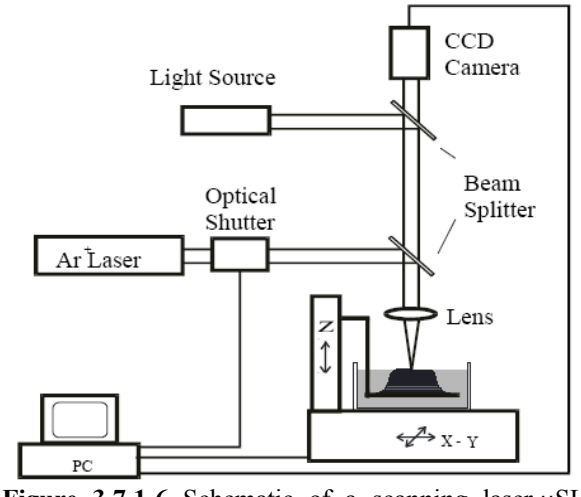

Figure 3.7.1-6 Schematic of a scanning laser μSL system [1].

Current state of the art

Conventional stereolithography (SL) was invented by Charles Hull of 3D Systems in 1984 as a rapid prototyping technology [1, 9]. Its goal was to allowed engineers to generate scale models of complicated three-dimensional parts in a fraction of the time and at a fraction of the cost of traditional methods. To this end, SL has been hugely successful at providing a tool for visualizing components and assisting in the iterative design process. In the realm of microsystems, SL can provide for both this design methodology and for direct production of functional parts and microdevices.

There are several methods for three-dimensional fabrication of microstructures using stereolithography. The most basic technique is a simple scanning laser system as shown in Figure 3.7.1-1. A typical setup of this kind uses a laser to serially trace the shape of the desired part in a line-by-line manner over the free surface of a polymer resin bath. When a layer is fully solidified under the exposure of a laser beam, the component stage drops down to allow a fresh layer of liquid polymer to flow over the solid surface. The laser is controlled by a CAD system that functions as an electronic mask and allows for a transverse resolution of ~150μm. In addition, the photopolymer can be loaded with ceramic, metal, or other particles to generate components of different materials. After initial stereolithographic fabrication, the parts can be sintered to remove the polymer and densify the functional material of interest. This usually shrinks the part by some controllable amount.

An advancement on this scanning laser technique is the Two Photon Absorption method. This process requires two low power, pulsed laser beams which intersect deep within the resin bath. At the intersection point, the beams form a small volume element which has enough photon flux to polymerize only the local material. The beams can then write a completely three-dimensional pattern into the resin bath[10,11]. This is the highest resolution three-dimensional microfabrication technique available to date; however, there are several key disadvantages. Namely, the available resins for this technique are severely limited due to the need for them to be highly transparent to the laser beams. In addition, this transparency requirement eliminates the possibility of loading the resin bath with ceramic or metal particles. Finally, because Two Photon Absorption is a linear "point-by-point" writing technique it can be extremely slow and does not scale well to large areas or quantity.

PμSL is a third technique which was first accomplished by using a set of photomasks to project a two-dimensional image onto the resin bath rather than a single spot. Although effective, this method required a large number of photomasks thus limiting the practical number of layers possible. Using a dynamically reconfigurable mask in the form of a Liquid Crystal Display (LCD) was first demonstrated by Bertsch *et al.*[12]. This dramatically reduced process time resulting in structures with thousands of layers, however, the LCD had some intrinsic drawbacks including large pixel sizes and low switching speeds.

Likely cost throughput

Cost for generating components with these techniques will be a function of two parameters; capital equipment and materials. The equipment costs associated with a simple small scale PμSL system is ~$100K. With the addition of a superlens and holographic capability this cost will approximately double. It is more challenging to estimate the equipment cost associated with a scaled-up version of the system as this will depend on how large an area is optimal for batch processing and scaling studies that have not yet begun. Materials costs associated with this technique can range from very inexpensive for the polymer resin materials (~$100s for liters of resin) to relatively expensive if nanoparticles of metals or other materials are suspended in the polymer (colloidal gold nanoparticles are typically ~$1000 per 500 mL).

Research Needs

1. What limits resolution of system (with and without superlens) and what is best achievable resolution?
2. Impact of metal and ceramic particles in resin. What materials are feasible? Is sintering required and what is the effect on the final geometry?
3. Holographic nanolithography has never been attempted in this configuration. How deep a structure can be fabricated with one hologram?
4. What limits the throughput/speed of system?
5. Modeling efforts will be required to compliment experiments and answer some research questions.

Development cost and schedule

The development time for this technology is approximately 3 years for a prototype with superlens and holographic capability. An additional 2 years will be needed to for scaling the system to wide area. The cost per year for the prototype system is approximately $750k; for the scaled up version, this cost is substantially more and is not estimated here. The table below summarizes this schedule.

	FY 09	FY 10	FY 11	FY 12	FY 13
Baseline PμSL	◄——►				
Superlens integration		◄——►			
Holographic nanolithography			◄——►		
Scale up				◄——►	——►

References:

1. Cox, A., Xia, C., Fang, N., "Microstereolithography: A Review," ICOMM, 2006, No. 55.
2. Xia, C., Fang, N, "3D microfabricated bioreactors," in press, 2007.

3. Sun, C., Fang, N., Wu, D.M., Zhang, X., "Projection micro-stereolithography using digital micro-mirror dynamic mask," *Sensors and Actuators: A Physical*, 121 (2005), pp 113-120.
4. Pendry, J.B., "Negative refraction makes a perfect lens," *Phys. Rev. Lett.*, 85, 3966-3969, 2000.

5. Liu, Z.W., Fang, N., Yen, T-J., Zhang, X., "Rapid growth of evanescent wave by a silver superlens," *Appl. Phys. Lett.*, 83, 5184-5186, 200
6. Fang, N., Lee, H., Sun, C., Zhang, X., "Sub-diffraction-limited optical imaging with a silver superlens," *Science*, 308, 534-537, 2005.
7. Liu, Z., Durant, S., Lee, H., Pikus, Y., Fang, N., Xiong, Y., Sun, C., Zhang, X., "Far-field optical superlens," *Nanoletters*, 2007.
8. Campbell, M., Sharp, D. N., *et al.*, "Fabrication of photonic crystals for the visible spectrum by holographic lithography", *Nature*, 404, pp. 53–56, 2000.
9. Jacobs, P.F., Stereolithography and other RP&M Technologies, ASME Press, 1996.
10. Kawata, S., Sun, H-B., Tanaka, T., Takada, K., "Finer features for functional microdevices," *Nature*, vol. 412, Aug. 16, 2001, pp. 697-698.
11. Sun, H-B., Kawakami, T., Xu, Y., Ye, J-Y., Matuso, S., Misawa, H., Miwa, M., Kaneko, R., "Real three-dimensional microstructures fabricated by photopolymerization of resins through two-photon absorption," *Optics Letters*, vol. 25, no. 15, August 1, 2000, pp. 1110-1112.
12. Bertsch, A., Jiguet, S., Hofmann, H., Renaud, P., "Ceramic microcomponents by microstereolithography," 17th IEEE Conference on MEMS, p. 728, 2004.

3.7.2 Electrophoretic Deposition

Process description

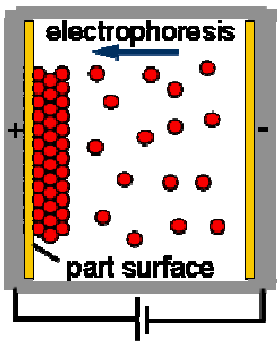

Figure 3.7.2-1. Schematic of the electrophoretic deposition process.

Electrophoretic deposition (EPD) is a directed particle assembly method which utilizes electric fields to deposit charged nanoparticles from a solution onto a substrate[1]. EPD requires the deposition substrate to act as one electrode to attract oppositely charged particles from the solution. This can be achieved on non-metal parts by coating the surface with a thin metal layer (order 100 nm thick). The part is then submerged in a conductive solution (solvent or aqueous) containing suspended nanoparticles of the desired coating material. The nanoparticle charge and size as well as the electric field strength determine the deposition rate and eventual coating thickness. These parameters can be controlled to provide precise coating thicknesses and the packing structure of the deposited particles. The coating is then stabilized through drying and/or sintering.

This is approach is proposed for coating a pre-fabricated polymer (or similar material) hohlraum with a 20 μm thick metal layer.

Current state of the art

EPD has been used with a wide range of nanoparticles including oxides [2-7], metals [8, 9], polymers [10, 11], semiconductors [12, 13], and even diamond [14]. The process can currently be used to synthesize cylindrical and other net-shape mm-scale parts [15], density and composition-gradient coatings and materials [16]. Coatings can be as thick as a few millimeters. The surface roughness is dependent on the particle size and other deposition parameters. The process is primarily used to deposit ceramic coatings on metals [17, 18], but several groups have demonstrated electrophoretic deposition of colloidal gold [19, 20]. Through an internally funded ENG project, researchers at LLNL demonstrated electrophoretic deposition of multilayer colloidal gold films using 30-80 nm precursor material.

Likely cost throughput

Cost will primarily be driven by the coating material. Suspensions of colloidal gold nanoparticles are typically ~$1000 per 500 mL and provide 1.2 mm^3 worth of material for this volume.

Research needs

1. Materials compatibility and deposition parameters will need to be determined based on the selected material for the hohlraum part and desired coating.
2. Process modeling will be necessary to ensure uniform coating thickness around the non-planar hohlraum shape. Corners and edges will generate electric field gradients which will increase particle-particle interactions during deposition. These interactions can be eliminated be altering field magnitudes based on the process model.
3. Drying and sintering of the proposed material must be analyzed as a function of thickness and deposition parameters. Optimized conditions will eliminate cracking and peeling due to internal stresses.

Development cost and schedule

The basic development of the process is estimated to require up to 2 years with a rough order of magnitude cost of $250k/year. Depending on the surface roughness metrics, additional development may be necessary, extending the development for an additional year at the same estimated cost.

	FY 09	FY 10	FY 11
Set up deposition system for hohlraum	◄——►		
Develop deposition process	◄———	———►	
Refine surface roughness			◄——►

References:

1. Besra, L. and M. Liu, *A review on fundamentals and applications of electrophoretic deposition (EPD).* Progress in Materials Science, 2007. **52**: p. 1–61.
2. Ferrari, B. and R. Moreno, *Zirconia thick films deposited on nickel by aqueous electrophoretic deposition.* J. Electrochem. Soc. , 2000. **147**: p. 2987-2992.
3. Tang, F., et al., *Electrophoretic deposition of aqueous nano-y-Al2O3 suspensions.* Mat. Res. Bull., 2002. **37**: p. 653-660.
4. Zanetti, S.M., et al., *$SrBi_2Ta_2O_9$ ferroelectric thick films prepared by electrophoretic deposition using aqueous suspension.* J. European Chem. Soc., 2004. **24**: p. 2445-2451.
5. Yui, T., et al., *Synthesis of photofunctional titania nanosheets by electrophoretic deposition.* Chem. Mater., 2005. **17**: p. 206-211.
6. Yamada, K., et al., *Insertion of SiO_2 nanoparticles into pores of anodized aluminum by electrophoretic deposition in aqueous system.* Electrochem. Solid State Lett., 2004. **7**: p. B25-B28.
7. Kruger, H.G., et al., *Composite ceramic-metal coatings by means of combined electrophoretic deposition and galvanic methods.* J. Mat. Sci., 2004. **39**: p. 839-844.
8. Li, H.X., M.Z. Lin, and J.G. Hou, *Growth of metal/organism multilayer films from ligand-stabilized silver nanoparticles.* J. Mat. Sci. Lett., 2000. **19**: p. 963-964.
9. Windes, W.W., J. Zimmermann, and I.E. Reimanis, *Electrophoretic deposition applied to thick metal-ceramic coatings.* Surf. and Coat. Tech., 2002. **157**: p. 267-273.
10. Velev, O.D. and K.H. Bhatt, *On-chip micromanipulation and assembly of colloidal particles by electric fields.* Soft Matter, 2006. **2**: p. 738-750.
11. Aizenberg, J., P.V. Braun, and P. Wiltzius, *Patterned colloidal deposition controlled by electrostatic and capillary forces.* Phys. Rev. Lett., 2000. **84**: p. 2997-3000.
12. Sun, J., M. Gao, and J. Feldmann, *Electric field directed layer-by-layer assembly of highly fluorescent CdTe nanoparticles.* J. Nanosci. Nanotech., 2001. **1**: p. 133-136.
13. Ordung, M., J. Lehmann, and G. Ziegler, *Fabrication of fibre reinforced green bodies by electrophoretic deposition of silicon powder from aqueous suspensions.* J. Mat. Sci., 2004. **39**: p. 889-894.
14. Affoune, A.M., et al., *Electrophoretic deposition of nanosized diamond particles.* Langmuir, 2001. **19**: p. 547-551.
15. Tabellion, J. and R. Clasen, *Electrophoretic deposition from aqueous suspensions for near-shape manufacturing of advanced ceramics and glasses – applications.* J. Mat. Sci., 2004. **39**: p. 803-811.
16. Uchikoshi, T., et al., *Dense, bubble-free ceramic deposits from aqueous suspensions by electrophoretic deposition.* J. Mater. Res., 2001. **16**: p. 321-324.
17. van der Biest, O.O. and L.J. Vandeperre, *Electrophoretic Deposition of Materials.* Annual Review of Materials Science, 1999. **29**: p. 327-352.

18. Baufeld, B. and O.O. van der Biest, *Development of Thin Ceramic Coatings for the Protection against Temperature and Stress Induced Rumpling of the Metal Surface of Turbine Blades.* Key Engineering Materials 2007. **333**: p. 273-276.
19. Kooij, E.S., et al., *Formation and optical characterisation of colloidal gold monolayers.* Colloids and Surfaces A: Physicochemical and Engineering Aspects, 2003. **222**: p. 103-111.
20. Giersig, M. and P. Mulvaney, *Formation of ordered 2-dimensional gold colloid lattices by electrophoretic deposition.* J. Phys. Chem, 1993. **97**: p. 6334-6336

3.7.3 Hollow Jet Instability Method

Process description

The fabrication of high quality amorphous metal microballoons with uniform shell thickness, low surface roughness, and high sphericity can be accomplished by exploiting the natural instability of a hollow liquid jet under free fall. It is well known that a falling liquid jet is naturally unstable with respect to "break up" into droplets. Under controlled conditions, spherical droplets with a narrow size distribution are formed when oscillations of the jet diameter grow with distance along the path of fall. Lee, Kendall, and Johnson[1] were able to produce uniform distributions of solid metallic glass spheres by allowing such droplets of Au-based metallic glass forming liquid to solidify during free fall in a drop tower. When the liquid droplets crystallize during fall, the sphere surfaces are rough and non-uniform due to the discontinuous nature of liquid-crystal phase transition which involves discontinuous changes in molar volume, enthalpy, etc. By contrast, when the cooling rate of the droplet during fall is sufficient to bypass crystallization, the undercooled liquid reaches the glass transition without crystallizing and metallic glass spheres are formed. These spheres were found to exhibit extremely smooth surfaces with roughness in the range of nm's. Examples of glassy and crystallized spheres are shown in Fig.3.7.3-1 (taken from ref.2).

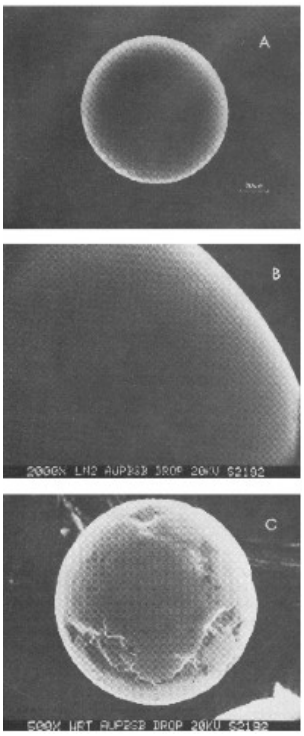

Figure 3.7.3-1 A) A ~100μm diameter sphere of metallic glass produce by free fall
B) Same as (A) at higher magnification
C) A crystallized sphere of similar diameter showing high surface roughness.

When the same liquid is forced to flow through a vertically oriented concentric orifice, a hollow jet is formed which again undergoes a growing oscillatory instability in its diameter along the path of fall. The jet ultimately undergoes a periodic "pinching off" and spherical balloons are formed. Using this Hollow Jet Instability Method (HJIM), Lee, Kendall, and Johnson were able to fabricate uniform microballoons with wall thickness of about 10-30 μm and balloon diameters

ranging from several hundred μm up about 2mm. These microballoons exhibit a narrow distribution of diameters, very low surface roughness (in the nm range), and a high degree of sphericity (< 1 % variation). Figures 1 and 2 show examples of the glass and crystalline spheres as well as a ~1mm diameter microballoon fabricated from an Au-based metallic glass forming alloy.

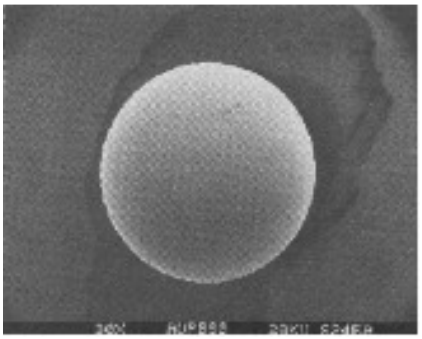

Figure 3.7.3-2 A metallic glass microballoon of diameter ~1mm and wall thickness of about 20 μm. Note high degree of sphererecity and low surface roughness.

The Au-based glass forming alloys used in the early work of references 1 and 2 were relatively poor glass formers with critical casting thicknesses of the order of 1mm or less. The critical casting thickness reflects the minimum cooling rate required to bypass the crystallization of the alloy and therefore reflects the "processability" of the alloys. Since the early work on microballoons, the Caltech group and other groups worldwide have developed several families of glass forming alloys with critical casting thicknesses ranging up to cm's.[3,4] These highly processable alloys would be better suited to the production of glassy spheres and microballoons in a drop tower set up. For LIFE capsules, it may be desirable, for example to fabricate microballoons from alloys containing metals which have low cross sections for neutron absorption. For example, Be and Zr are two such metals.

Over the past ten years, the Caltech group has developed a large family of bulk glass forming alloys based on the metals Be and Zr. In particular, recent work has focused on Zr-Ti-Be, Zr-Cu-Be, and other related glass forming alloys[5,6,7]. In fact, these alloys exhibit critical casting thicknesses ranging from mm's to cm's. They are highly processable and would be ideal materials for fabrication by HJIM.

Scale-Up, High Rate Production, and Gas Encapsulation

The HJIM method lends itself to high rate production of large quantitites of microballoons. The natural production rate of microballoon shells would be in the range of tens of balloons per second for balloon size in the mm range. The process could be carried out on a continuous basis for extended time intervals enabling the production of millions of samples per day within a single facility. An actual facility would produce balloons with a finite but narrow distribution of diameters. These balloons could be further "sieved" or sorted by size to achieve narrower distributions. By varying the parameters which control the hollow jet (orifice geometry, liquid flow rate through the orifice, etc.), one may achieve variable wall thickness in the microballoons. These issues would require further investigation and modeling to determine the characteristic distribution functions for a given HJIM process.

If the drop tower contains a gas at ambient pressure, the gas will naturally be entrained in the balloons as they are formed. If the drop tower is designed to allow overpressure

containment, the device would produce balloons containing elevated pressures (above 1 atm.) of the gas which fills the drop tower vessel.

Development cost and schedule

The basic development of the process including the jet and drop tower is estimated to require up to 2 years with a rough order of magnitude cost of $200K/year. Refining the surface roughness and geometric properties as well working with new materials will require an additional 1-2 years at ~$150K/year. Process scale-up will occur in year 5 at a cost of ~$250K.

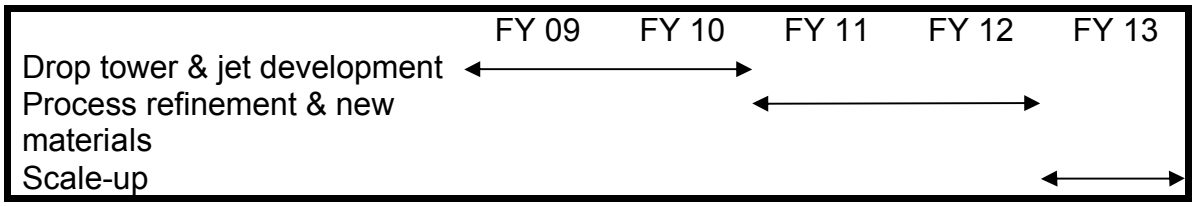

References:

1. W.L. Johnson and M.C. Lee, "the Use of Metallic Glasses in Fabrication of ICF Targets", J. Vac. Sci. & Tech. A, 1, 1568 (1983).
2. M.C. Lee, J.M. Kendall, and W.L. Johnson, "Spheres of the Metallic Glass Au-Pb-Sb and their surface characteristics", Appl. Phys. Lett. 40, 382 (1982).
3. A. Inoue, "Stabilization of metallic supercooled liquid and bulk amorphous alloys", Acta Mater., 48, 279 (2000).
4. W.L. Johnson, "Bulk glass-forming metallic alloys: science and technology", Mat. Res. Soc. Bulletin, 24, 42 (1999).
5. A. Wiest, G. Duan, M.D. Demetriou, and W.L. Johnson, "Zr-Ti-based Be bearing glasses optimized for high thermal stability and thermoplastic forming", Acta Mater., 56, 2625 (2008).
6. G. Duan, A.Wiest, M.L. Lind, and W.L. Johnson, "Lightweight Ti-based bulk metallic glasses excluding late transition metals", Scripta Mater., 58, 465 (2008).
7. G. Duan, M.L. Lind, K. de Blauwe, and W.L. Johnson, "thermal and elastic properties of Zr-Be-Cu bulk metallic glass forming alloys", Appl. Phys. Lett., 90, 211901 (2007).

4.0 Target Injection

Description and Specifications

Targets are received from fabrication and layering, loaded into an accelerator, accelerated to the required injection speed, possibly steered to improve accuracy, and tracked to provide final beam pointing and triggering information. Requirements and specifications for the injection system are listed in Table 4.1-1. Desirable features for a target injection system include low cost, reliability, easy maintenance, minimal perturbation of target design and reasonable development costs.

Table 4.1-1. *Requirements and specifications for a fast ignition target injection system.*

Base Requirements	**Specification**
Injection rate	13 to 20 Hz
Placement accuracy	1 mm (0.1 mrad at 10 m)
Target axis alignment (tumble)	10 mrad
Cone tip tracking accuracy	20 μm
Cryogenic Compatibility	Does not overheat target - especially DT fuel
Derived requirements	
Injection speed	130 to 200 m/s (50% of interpulse time in 5 m radius chamber)
Rotational speed	<400 rev/s (~6300 m/s^2 centripetal acceleration)
Injection acceleration	10,000 m/s^2 (Max for 18 K - higher may be acceptable with lower temperature targets)
Acceleration distance	2 m (for 200 m/s at 10,000 m/s^2)

There are several potential mechanisms for fast ignition target injection. These include the conventional magnetic accelerator, rail gun, gas gun, and induction accelerator.

The **conventional magnetic accelerator**, illustrated in Figure 4.1-1, energizes electrical coils in front of a ferromagnetic sabot insert.

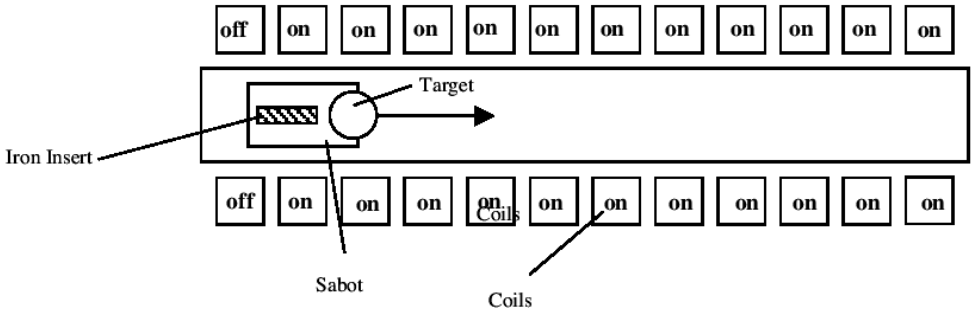

Figure 4.1-1 *The conventional magnetic accelerator pulls the target with energized coils.*

The **rail gun**, illustrated in Figure 4.1-2, passes current along rails and through electrically conducting material (armature) in the target. The armature current interacts with the magnetic field from the rail current to produce a force that propels the target.

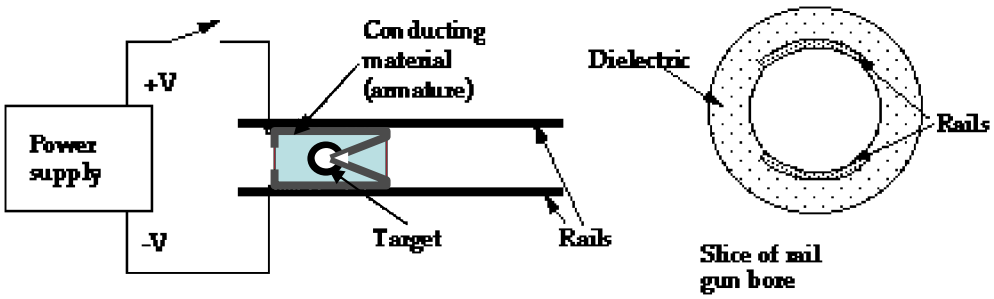

Figure 4.1-2 *The rail gun is the simplest electromagnetic accelerator.*

The **gas gun**, one concept for which is illustrated in Figure 4.1-3, utilizes gas pressure to propel the target down the gun barrel. A fast acting gas valve controls low atomic weight propellant gas such as hydrogen or helium.

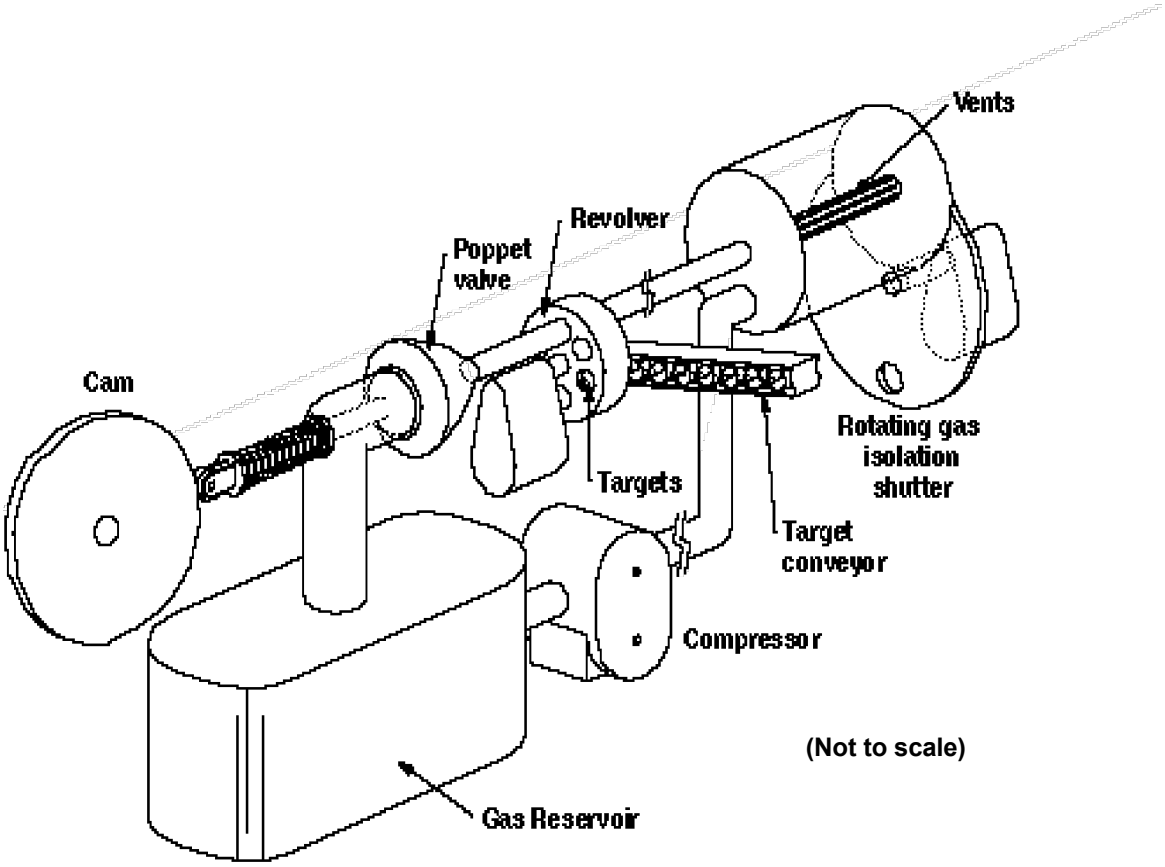

Figure 4.1-3 *The gas gun utilizes gas pressure to propel the targets.*

The **induction accelerator**, illustrated in Figure 4.1-4, utilizes several current carrying coils with inputs from a multiphase power supply to produce a traveling magnetic wave. This traveling wave induces a current in a conducting sleeve (armature) of the target. The induced current interacts with the magnetic wave to produce the propulsive force.

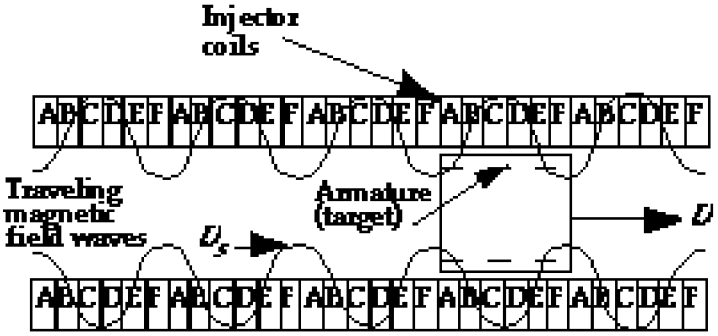

Figure 4.1-4 *The traveling wave in an induction accelerator induces circumferential current in the target with a resulting propulsive force.*

Additional injection mechanisms that are considered not viable for LIFE targets include electrostatic acceleration, which can only provide sufficient force for very low-mass direct drive targets, the "magnetic slingshot" (proposed for the direct drive IFE program) which has a maximum speed of about 60 m/s, and mechanical injection methods that have a maximum speed of about 50-100 m/s.

4.2 Current state-of-the-art (abilities, advantages, disadvantages)

Indirect drive target injection experiments conducted at Lawrence Berkeley National Laboratory using a gas gun achieved 2 mm accuracy (1 σ) at 3 m standoff with a velocity of ~80 m/s. 10 mrad tumble (1 σ) was achieved with 200 rev/s spin in the same experiments.

Direct drive target injection experiments were carried out at General Atomics. A gas gun achieved 10 mm accuracy (1 σ) at 17 m standoff at 400 m/s. A reprate of 6 Hz was achieved for short burst operation using a revolver-based feed mechanism. A mechanical injector achieved 0.2 mm accuracy (1 σ) at 4 m with 300 mg spheres at 50 m/s (extrapolates to ~1 mm placement accuracy at 17 m, for comparison to the gas gun). Using in-flight target steering, better than 10 μm repeatability (1 σ) was achieved in each transverse direction by electrostatically steering ~1 mg spheres at 5 m/s with 0.5 m standoff from the steering electrodes[1]. For target in-flight tracking, 50 μm accuracy (1 σ) was achieved hitting surrogate targets on the fly with a low energy laser beam and ~3 m standoff to the steering mirror.

[1] While the 0.5 meter standoff is sufficient for some inertial fusion experiments, or perhaps sufficient for initial single-shot operations in a fusion test facility, it is not considered a sufficient standoff distance for an IFE power plant, i.e., we do not consider that the target can be steered into position for a power plant – rather that the beams will be steered to meet the target.

The acceleration methods require modifications that add material and mass to the LIFE target. The rail gun and induction accelerators require additional conducting sleeve material. The gas gun requires a material (such as membranes) to keep the warm gas away from the target cone and capsule and a material such as plastic to reinforce the outer wall of the hohlraum. In addition to an outer sleeve, finite element calculations show that additional material is required on the ends of the sabot to survive the required acceleration. The sleeve is illustrated in Figure 4.2-1 and example thickness with resulting target mass values are listed below.

Base target with 20 μm Pb	= ~0.2 g
Target with 0.2 mm polymer (gas gun or conv. mag.)	= ~0.4 g
Target with 0.4 mm Li (induction or rail gun)	= ~0.4 g
Target with 0.4 mm Pb (induction or rail gun)	= ~3 g

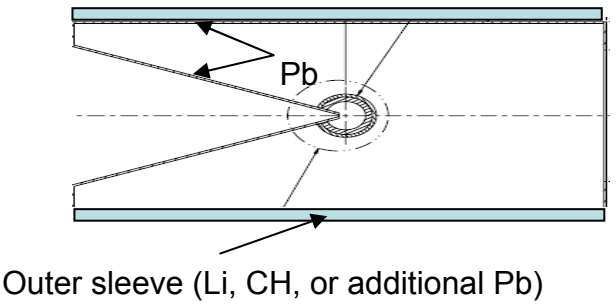

Figure 4.2-*1 An outer sleeve may be added to the target electrical conduction and/or structural support.*

The conventional magnetic accelerator has the advantages of causing a relatively small amount of target heating and requires less modification of the target. However, it does require a sabot to carry the target, that should not go into the reaction chamber and this requires in-flight separation. This sabot makes the physical contact with the barrel. Accuracy may suffer because the target is effectively released from the very short "barrel" of the sabot.

The rail gun probably would not work with a Pb armature because the density of Pb is high and the electrical conductivity of Pb is just moderate. Approximately 8.7 kA of current would be required to achieve 10,000 m/s^2 acceleration. With 0.24 mΩ resistance the temperature of the Pb would increase to greater 500 K. The minimum contact resistance that is achievable is unknown, but may well be much greater than 0.24 mΩ and cause an even greater temperature rise. Utilizing a Li sleeve, the required current would be reduced to ~3.2 kA and the temperature rise (neglecting contact resistance) would be ~16 K. A major concern for a rail gun is that a conducting lubricant such as MoS_2 or eroded material from the targets could cause short circuits between the rails. We don't believe that the rail gun is a good choice for a LIFE injector because of the likelihood of low reliability.

A gas gun is a simple proven device for accelerating room temperature projectiles but requires warm gas that will heat the target and has to be differentially pumped to prevent it from entering the reaction chamber. Finite element calculations show that target heating would be much too large if the gas is allowed to come into contact with the target cone and capsule. Figure 4.2-2 shows the temperature profile in the capsule and DT based on conduction from 1 MPa of 300 K He gas for 20 ms. The gas gun also requires contact between the target and the barrel that would cause barrel wear and could present a problem with thermal expansion of the target into the barrel walls.

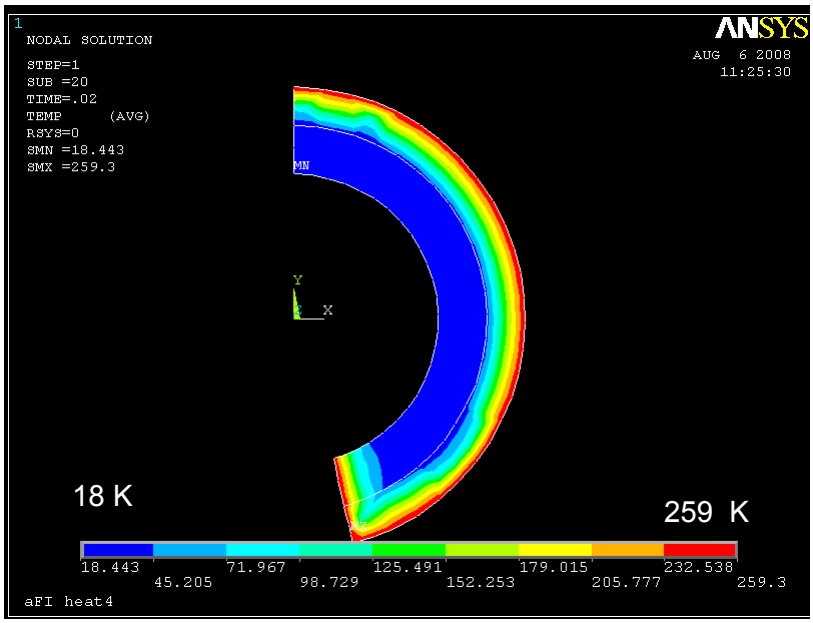

Figure 4.2-2 *Temperature distribution after 20 ms with 300 K He gas.*

Thermal protection for the fuel will be needed. For example, membranes might be placed at the entrances to the cone and hohlraum. A lower thermal conductivity material than Pb might be needed to avoid a heat short to the fuel.

The induction accelerator addresses some of the issues of the rail gun (and gas gun). There is no electrical contact between the barrel and the target. There is also a centering force such that physical contact between the barrel and target might be avoided. As with the rail gun, much less current and armature heating result if the target sleeve is made of Li than with Pb. Preliminary calculations assuming the 100 K material properties suggest that a Pb target would require a 430 kVA ~15 kHz variable frequency power supply for each phase and have a final sleeve temperature >370 K to achieve 200 m/s. Similar calculations suggest that a Li sleeve target would require a 17 kVA ~12.5 kHz variable frequency power supply for each phase and have a final sleeve temperature ~55 K to achieve 200 m/s. However, integrated calculations utilizing temperature dependent material properties indicate that a lower slip speed is desirable at cryogenic temperature and that a smaller temperature rise results for both the Pb sleeve and for the Li sleeve.

Target steering (after leaving the barrel) should substantially improve placement accuracy for injected targets. The targets would be electrically charged, tracked and run through charged steering electrodes to correct measured trajectory errors prior to entering the reaction chamber.

Table 4.2-1 compares how well above the target injection methods would meet our requirements. The gas gun and induction accelerator are top contenders, but both still have issues.

Table 4.2-1. *Accelerator methods checklist*

Requirement/ Parameter	Injector Requirements	Conv. Magnetic	Railgun	Gas gun	Induction
1. Repetition Rate (Hz)	13 - 20	+	+	0	+
2. Acceleration (m/s^2)	10,000	+	+	+	+
3. Injection speed (m/s)	130-200	+	+	+	0
4, Target axis alignment (mrad)	10	?	?	+	?
5. Cryogenic compatibi lty		+	0	0	0
6. Target Spin (rev/s)	Up to 400	0	0	+	+
7. Target Accuracy (mrad)	± 0.1	-	?	0	?
8. Cost		0	+	0	+
9. Reliability/wear		0	-	0	+
10. Minimal perturbation to target design		+	-	0	0
11. Development cost		0	0	+	0
Score		+4	+2	+5	+5

4.3 Target heating issues and mitigation

Pb vapor in the chamber could excessively heat the cone and capsule (even if the vapor pressure equaled the 1000 K operating temperature and is not ionized). The vapor pressure of Pb between 550 and 1000 K is given by

$P_{Pb} = 1.5 \times 10^{10} \exp(-22900/T)$ Pa (Ref.1)

for 1000 K the vapor pressure is 1.7 Pa. The number density of Pb particles is

$$\frac{n}{V}=\frac{P}{RT}=\frac{1.7\text{Pa}}{(8.3\text{J/mole}\cdot\text{K})(1000\text{K})}=2.0\times10^{-4}\text{moles/m}^3=1.3\times10^{14}/\text{cm}^3$$

The number of moles per unit area of Pb contained in a 5 m target transit path length is then

$$\frac{n}{A}=1.0\times10^{-3}\text{moles/m}^2$$

The thickness of a condensed layer with this mole density is

$$T=\frac{n(MW)}{A\rho}=\frac{10^{-3}\text{moles}}{\text{m}^2}\frac{0.207\text{ kg}}{\text{mole}}\frac{\text{m}^3}{11{,}000\text{ kg}}=18.8\text{ nm}.$$

This is enough Pb to reflect and absorb a large fraction of the laser light. However, since only about 19 nm of Pb is deposited, it likely would not have enough energy to melt a micron or greater thickness membrane.

The thermal energy in 10^{-3} moles of Pb at 1000 K is roughly

$$E=(30J/mole\cdot K)1000K=30kJ/mole=30J/m^2$$

The heat of vaporization of Pb is 178 kJ/mole, so the total heat released is roughly 210 kJ/mole or 210 J/m^2. If deposited on a cone with a 30° cone angle, the thickness is reduced by the tangent of 15° = 0.27 for a total of 5 nm. The heat capacity of Pb at 18 K is about 8 J/mole•K, so the temperature rise of the cone would be

$$\Delta T=\frac{5nm}{20\mu m}\frac{210kJ/mole}{8J/mole\cdot K}=6.5K.$$

The associated heat flux from the Pb deposition on the cone is ~52 J/m^2 delivered in 25 ms = 2080 W/m^2 or about 0.2 W/cm^2.

The black body heat load at 1000 K is 5.7 W/cm^2. There are several factors that must be considered regarding the radiation heat load in the cone. The first reflection rays deep inside the cone approach the surface with an angle of incidence between ~60° and 90°. However multiple reflections can occur with larger angles of incidence increasing the heat absorbed before the remaining light is reflected back out of the cone. The net heating effect of these multiple reflections need to be calculated. A highly reflective surface will be needed.

Xenon gas with density of 3*10^{16}/cm^3 is intended to be included in the chamber to protect the chamber walls. This is ~200 times greater than the calculated Pb density. D2SV Monte Carlo code heat flux calculations were accomplished for direct drive targets passing through Xe gas at 200 m/s with the following results for 3 different xenon densities.

1.6*10^{14}/cm^3 gives 0.046 W/cm^2
1.6*10^{15}/cm^3 gives 0.41 W/cm^2
1.6*10^{16}/cm^3 gives 1.3 W/cm^2

As the density increases there is a self-shielding effect of the gas. Similar calculations should be done for the LIFE target. It is possible that greater self-shielding would occur as atoms are trapped in the cone. The Xe gas could also shield some of the Pb atoms from reaching the cone, but could also interfere with Pb atoms condensing and being removed from the chamber.

Concepts for reducing the heating of the cone and capsule include installing membranes at the opening of the cone and hohlraum and installing insulation between the cone and DT fuel layer. One could investigate the feasibility of using a heat shrink and or scored polymer membranes that could fracture and retract from the beam path as it is heated in the chamber.

4.4 Research needs (technical, cost, schedule)

Research needs include needs such as:

- Chamber conditions must be better known to further define the injection conditions, effects on the target, and target modifications needed for target survival. Chamber gas affects target heating and trajectory. Important parameters include composition, density, temperature, ionization, and velocity.
- Target heating calculations must be carried out for both conditions of (a) in the accelerator and (b) in the chamber. The effect of thermal expansion in the accelerator must be determined. As chamber conditions become better understood, they can be used for the heating calculations. Prior to attaining this information, calculations can be performed for a range of chamber conditions. Methods to reduce target heating such as membranes and insulation will be evaluated.
- Target spin will almost certainly be required to keep the target axis aligned with the driver beams. Utilizing a rotating magnetic field to induce this spin should be investigated with both theory and experiment.
- Cryogenic target handling and loading methods need to be developed.
- An induction accelerator prototype should be designed and a prototype built and tested, first at the laboratory scale. Cryogenic operation may be necessary to demonstrate operation with high electrical conductivity and the resultant low critical slip speeds.
- A lab-scale gas gun needs to be developed for use with cryogenic targets. Cryogenic target handling, thermal heating and thermal expansion mitigation methods need to be developed.
- Accuracy testing and improvement with target steering should be implemented.
- Target tracking methods and features must be tested. A rotating reflector near the barrel with a hole for target passage has been proposed to direct a Poisson-spot tracking beam to a camera. In the case of a gas gun, the rotating reflector would be downstream of the differential pumping chambers. Measurement fiducial concepts should be tested as well as added target features required for glint operation.
- In addition to testing target injection features, any target modifications required for target injection must be verified compatible with the rest of the power plant requirements. Methods for mass-producing these modified targets must be developed.
- The neutron damage effects and mitigation methods should be evaluated.

- After proof of principle testing has been completed, further development will be required to optimize the chosen methods' performance and reliability. The goal of this work is develop target injection and tracking to be ready for integration into a prototype power plant design.
- A proposed timeline for the above mentioned research is given in Table 4..4-1. The estimated cost for this research is 3 FTE's/yr for 5 yr plus $2.5 M for capital-equipment purchases. All research items listed are important, but the most critical items that effect the LIFE concepts viability and affect the required target modifications that will be needed are chamber conditions studies and the resulting effect on target heating.

Additional information is shown below.

- Figure of merit : Placement accuracy and tumble, target survival, tracking accuracy
- Cost per target :~$0.005
- Throughput : 13-20 targets/s
- Current specs :10 mrad tumble, 1 mm placement, 20 μm tracking accuracy
- Risks : Currently unknown chamber conditions, untested injection concept, sufficient tracking accuracy not yet demonstrated
- Probability of success : High
- Process development cost : 4 FTE/yr X 5 yr + $2.5 M for initial research items

Table 4.4-1. *Target injection research program timeline.*

	FY 09	FY 10	FY 11	FY 12	FY 13	FTE years
Evaluation of target injection concepts implications for target and plant design eg. Li in Pb target	←	→				1
Chamber conditions calculations	←	→				1
Target heating calculations	←	→	→			1
Magnetically induced spin	←	→				1
Induction accelerator prototype (lab-scale)	←	→	→			2
Gas gun prototype (lab-scale) for cryogenic targets		←	→	→		3
Injection accuracy tests Including target steering		←	→	→	→	2
Target tracking methods	←	→	→	→	→	2

and features						
Target handling and loading methods			←	—	→	3
Neutron damage effects and mitigation				←	→	1
Optimization development for performance and reliability				←	→	3

References:

1. S. J. Zinkle, Summary of Physical Properties for Lithium, Pb-17Li, and (LiF)n•BeF2 Coolants, APEX Study Meeting, Sandia National Lab, July 27-28, 199
2. Petzoldt, R. *et. al*., "Target injection with electrostatic acceleration", TOFE Meeting, San Francisco, CA. September 2008.
3. Frey, D.T. *et. al.* , "Rep-rated target injection for inertial fusion energy", *Fusion Science and Technology*, 47 (2005) 1143-1146.
4. Petzoldt, R. W. and Jonestrask, K., "IFE Tracking and position update", *Fusion Science and Technology*, 47 (2005) 1126-1130.

5.0 Recovery and Recycle

5.1 Process Description

The recovery and recycle parts of the target lifecycle are shown in Figures 2.0-2 and 5.1-1. Following implosion, some parts of the targets will be vaporized and swept from the chamber and parts and materials will be deposited on the inside of the chamber walls. A ~1 torr xenon gas atmosphere will be sustained in the reaction chamber which will be continuously evacuated at a rate corresponding to the target ignition rep-rate. Vaporized target material will be swept along with the Xe gas and presumably deposited in the cold trap preceding the vacuum pump. Liquid or solid metals such as lead or gold may be found in the amalgam along with deposits of hydrocarbon material from the capsule. Particles impacting the chamber wall will experience the 700C wall temperature. Target materials may accumulate on the chamber walls in solid or liquid form. The target materials will be activated by the neutron flux generated during the implosion process. Following recovery of the activated materials from the chamber walls and the cold traps, the material will be set aside to "cool-down" or become less radioactive so that it can be handled. Many materials require a period of several days before it is acceptable for them to be returned to a processing line with shielded remote-handling capabilities. Select materials such as lead, in particular, can be stored for 2 years during which time it will become deactivated sufficiently to permit manual handing.[1] A summary chart of some candidate target materials and their properties are listed in Table 5.1-1.

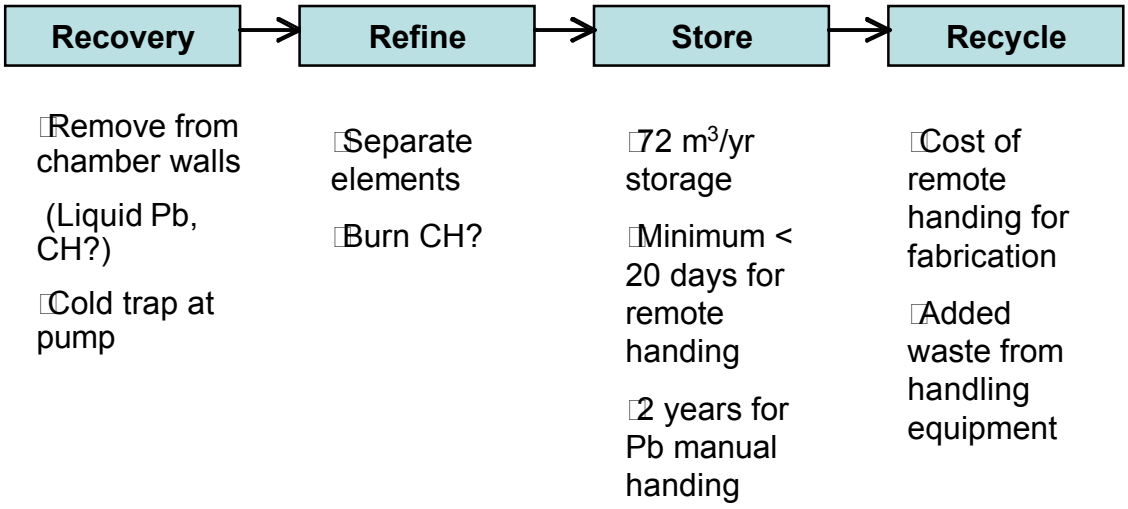

Figure 5.1-1 *Recovery-recycle process flow*

Table 5.1-1 *Select properties of candidate target materials*[1]

Material	Melting Pt (K)	Boiling Pt (K)	Wait time for remote handling	Wait time for manual handling	Dose products
Hg	234	630	5 days		^{202}Ti,^{196}Au,^{203}Hg
Pb	600	2022	13 days	2 years	^{203}Pb,^{202}Tl
Au	1337	3129	12.2 days		^{196}Au
Be	1560	2743			
Ta	3290	5731	1 day		^{182}Ta^{179}Hf
W	3695	5828	6.2 days		^{184}Re

The decision to recycle material rather than to simply dispose of the material will depend on costs and the acceptability of waste generation. Gold, for example, is a high-Z material being considered for the inner layer of the hohlraum. The price of gold is high enough, however, that even a thin, 0.02 mm layer on the inner diameter of the hohlraum is unacceptably expensive for consideration unless the material is recycled. Gold can be recycled with the caveat that the recycled materials will be radioactivate and remote handling equipment will be required in the target fabrication line. The costs for manipulating radioactive material must be factored into the target fabrication costs. If activated material is recycled into the hohlraum, not only the hohlraum fabrication tooling will be affected but all downstream assembly operations, DT layer formation and injection equipment will be affected as well. Costs for remote handling of radioactive materials could be as much as ten times the normal costs for fabrication.

5.2 Current State of the Art

Remote handling system technology is well within the state-of-the-art so if there is a need to build these systems, it is likely that they can be built with relatively little technical risk. Likewise, cold traps on pumps have been used ubiquitously, although potential corrosion issues from exposure to liquid metals will have to be addressed. Almost nothing is known about where target debris will deposit on the chamber walls and how the walls can be cleaned in-situ. Liquid metals and liquid lead, in particular, are corrosive. Research has to be conducted to find methods for corrosion resistance against liquid lead which is able to leach certain elements such as chromium from steels. The literature suggests that oxides can protect against leaching provided sufficient oxygen is in the lead to prevent destruction of the oxide coatings.[3]

A theoretical analysis of the activation products expected as a function of time and process history should be possible and would be useful to establish the feasibility of multiple use of the target materials.

5.3 Throughput and Costs

The amount of hohlraum material is likely to be about 72 cubic meters per year. A two-year supply of this material waiting to be cooled is well within a feasible storage volume. Organics may be incinerated although environmental issues concerning the vaporous tritium and other activated products must be addressed. The exact costs for handling and re-processing this material are unknown at this time.

5.4 Research Needs

Little is known about the areas of material recovery and reprocessing. Research topics include:

- Design of methods for removing material from chamber walls and pump cold traps.
- Development of suitable corrosion-resistant wall material.
- Study of recycled activated target materials to predict the composition following multiple uses of the material
- Design of separation processes for target materials
- Design of a remote handing system for activated target material and cost estimates for this system

Recovery and Recycle Development Plan

	FY 09	FY 10	FY 11	FY 12	FY 13
Recover					
Build prototype wall recovery system	←	—	→		
Build prototype pump recovery system			←	—	→
Refine					
Develop separation process	←	—	→		
Store					
Determine activation lifecycle	←	→			
Design prototype storage	←	—	→		
Recycle					
Design production recycle facility			←	—	→

References:

1. El-Guebaly, L., Wilson, P., Henderson, D., Varuttamaseni, A., "Feasibility of target material recycling as waste management alternative", *Fusion Science and Technology* 46 (2004) 506-518.
2. Reyes, S., Latkowski, J., Cadwallader, L.C., Moir, R. W., Gomez del rio, J., Sanz, J., "Safety issues of Hg and Pb as IFE target materials: Radiological versus chemical toxicity", Fusion Science and Technology, 44 (2003) 400-404.
3. Glasbrenne, H., Konys, J., Mueller, G., Rusanov, A., "Corrosion investigatins of steels in flowing lead at 400C and 550C", *Journal of Nuclear Materials*, 296 (2001) 237-242.

6.0 Target Cost

Based on the analysis conducted in the previous sections, the estimated per-target costs are summarized in Table 6.0-1 below. It can be seen from the table that the per-target costs are likely to meet the objective of about ~ $0.25/target provided that the high-throughput manufacturing techniques can be made to work for the target design.

Table 6.0-1 *Costs per target*

Item	**Sub-total**
Material (CH/Pb)	.01
Hohlraum/ cone	.04
Capsule/foam	.06
Assembly	.01
DT fill and layer	.07
Temperature control	.005
Injection, tracking	.006
Recover-recycle	.02
Facility charge	.01
Total cost	**$.231**

An estimate of the change in cost as a function of target production volume is based on a chemical engineering technique wherein the per-unit costs for the mechanical processes such as molding and stamping decrease with increasing volume at an exponential rate of 0.9 and chemical batch process such as micro encapsulation or extraction change at an exponential rate of 0.6. The equation for the price per target as a function of rep-rate is:

$$PPT(\nu) = M_0 + A_0\left(\frac{\nu}{\nu_0}\right)^{0.9-1} + B_0\left(\frac{\nu}{\nu_0}\right)^{0.6-1}$$

where:
PPT is the price per target in ¢/target,
ν is the rep rate in Hz and ν_0 is frequency in Hertz of base case [20 Hz]
M_0 is base case of material cost per target (¢/target) [0.278 ¢/target]
A_0 is base case of the cost of mechanical processes per target (¢/target) [6.0 ¢/target]
B_0 is base case of the cost per target of chemical processes (¢/target) [15.16 ¢/target]

Figure 6.0-1 shows a graph of the range of costs for target production volumes associated with rep-rates ranging from 5 Hz to 30 Hz. The estimated target cost ranges from $0.33 at 5 Hz to $0.21 at 20 Hz.

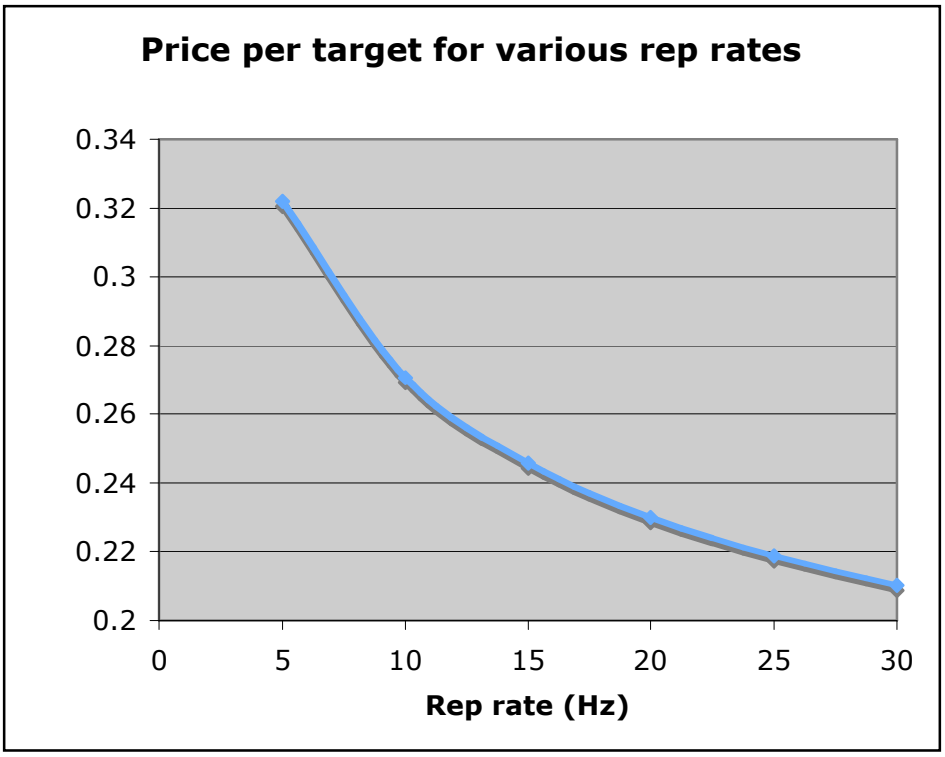

Figure 6.0-1 *Graph of cost variation with rep-rate*

7.0 Research Plan

The LIFE plant is not expected to produce power commercially for another 30 years. Between now and then many technical issues will have been resolved and demonstrations will have proven the viability of the LIFE reactor concept. The first steps in this process are the demonstration of ignition expected on NIF in 2010, a scoping design outlining a credible LIFE design scenario and a preliminary cost analysis to establish commercial feasibility. There are three major components to the LIFE system: the laser system, the fuel-power life-cycle and the target life-cycle. Much of the laser system technology is known as a result of the substantial investment in NIF although improvement of the optic's lifetime and reduction of diode costs remain challenges. Some of the fuel-power cycle technology is known from commercial reactors. Much fusion specific technology is still developmental. Most of the commercial fusion target technology is unknown. First, ignition has not yet occurred. This is the first step to characterizing the specific yields of the various target designs and better defining the allowable manufacturing tolerances. Second, targets made to date have been made at costs of about $100,000 each using labor and time-intensive precision manufacturing techniques. Successful LIFE targets must be made for ~$0.25 using techniques normally employed for low-accuracy consumer products like toys. Thirdly, the cold, fragile target must be injected at a velocity of up to 500 m/sec into the chamber with hot gas moving at about the same velocity in a direction possibly transverse to the target and the target must arrive within 1 mm of the implosion point in specific orientation with its structure and DT ice layer intact. Needless to say, this will be a significant technological challenge. Lastly, the imploded material must be collected and reprocessed in its now activated state.

In this report we have conducted a preliminary analysis of the issues surrounding the target life-cycle with emphasis on fabrication, injection and recycling. An extensive research program will be required to surmount the technical challenges of the target life-cycle. Key technology issues for each of the areas are listed in Table 7.0-1. A timeline for the demonstration of the key technologies needed to design the prototype target system is shown in Table 7.0-2. The projected research costs are shown in Figure 7.0-3. Because there is significant uncertainty in the optimal techniques for fabrication, multiple paths may be pursued initially with a down-select process occurring following the initial investigations. This is particularly true of the capsule and foam fabrication as shown in Table 7.0-2 where a down-select occurs at the end of year 3. It should be recognized that the target system design is itself a moving target as revelations in one part of the cycle emerge and impact the work on another part of the cycle. For example, if the induction technique for target injection requires a high-conductivity jacket on the hohlraum, this new requirement will affect the target design, fabrication and recycling efforts. Use of beryllium capsules or embedded dopants within the capsule walls require consideration of completely different fabrication technologies than the baseline homogenous plastic capsules discussed in this report. The cost to demonstrate the key technologies needed to design the prototype target system is estimated to be about $51.2M over a period of 5 years.

Table 7.0-1 *Key target technical challenges*

Target sub-system	Key technical challenges
Fabrication	
Hohlraum/cone	Achieve dimensional specifications using high-throughput manufacturing methods
Capsule	Achieve dimensional specifications using high-throughput manufacturing methods
Foam	Develop method to mold inside capsule
	Achieve high yield for micro-encapsulation technique
DT layer	Determine of DT will stay in foam and not crack
	Verify acceptability of possible cracks in foam
Injection/tracking	Determine survive-ability of target in injector
	Achieve accurate injection despite gas flow
	Tracking of target in reactor vessel
Recovery-recycle	Develop recovery techniques for target residuals
	Develop separation techniques for target residuals

Table 7.0-2 *Timeline for target research program*

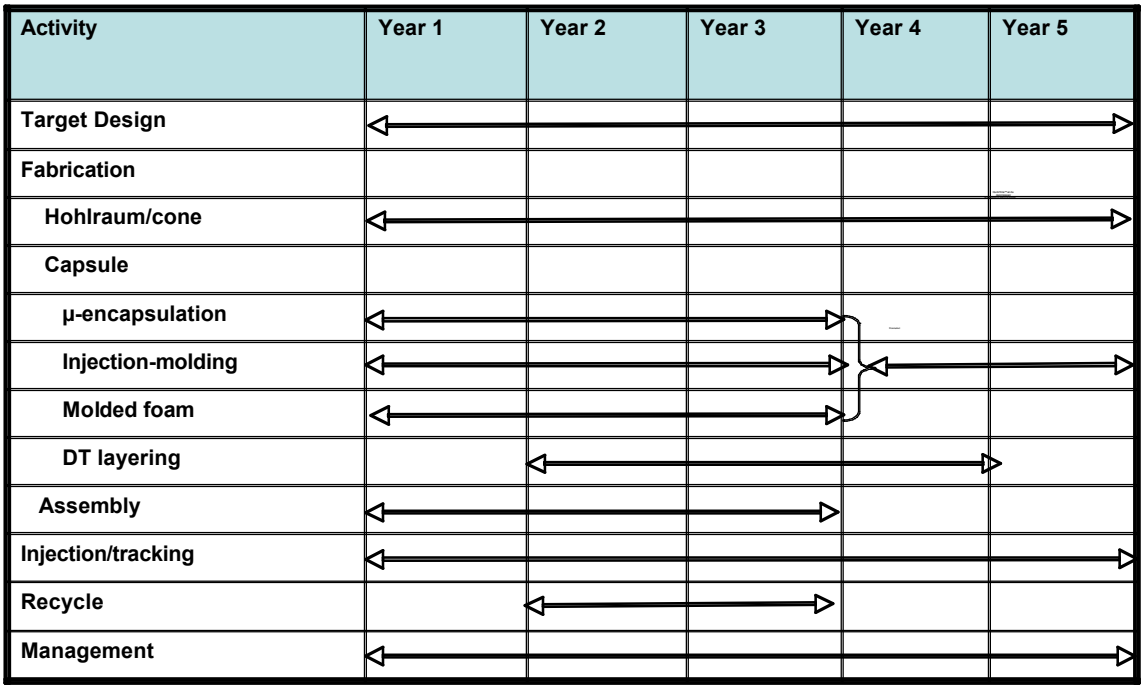

Table 7.0-3 *Costs for target research program*

Activity	FTE	Supplies ($M)	Dev. Time (Years)	Est. Dev Cost ($M)
Target Design				
Fabrication				
Hohlraum/cone	4	2	5	9
Capsule				
μ-encapsulation	5	2	5	10.75
Injection-molding	4	2	3	6.2
Molded foam	3	.5	3	3.65
DT layering	3		3	3.15
Assembly	2	1	3	2.1
Injection/tracking	4	2.5	5	9.5
Recycle	1		2	0.7
Management	3		5	5.25
Total Estimate	30	10		50.3

9.0 Conclusion

The forgoing study concludes that the LIFE fast ignition targets could possibly be built at high enough production rates and low enough cost to result in a commercially feasible LIFE plant. Even the specifications for the fast ignition target which are about an order of magnitude less stringent than those for the current hot spot design are challenging enough to require a demonstration to verify the claim of low target fabrication cost, inject-ability and recycle-ability. This demonstration will be the result of the research program that has been outlined here. The research program is estimated to require 5 years at about a $10M/year funding level. At the end of this research program we will have the confidence to go forward with the pilot production plant, a big step in making fusion energy a viable option.

Appendix A: Costing Method for Capsule Fabrication

To determine the capsule costs for different processes, the first step was to define all of the process steps required to complete the capsule. Once all of the process steps were identified, the material balances were calculated to determine the flow rates of chemicals at each step. From this information, the equipment sizes and required number of units were determined.

The material balances and equipment sizes are strongly influenced by the rejection rate of the shells at quality analysis/control steps, so projections of the expected rejection rates for each process type were made. Before process steps requiring high equipment or materials expenditures (such as GDP-coating steps), additional QA/QC steps were included to reduce the equipment size and materials consumption that would be required to account for a larger flow rate of capsules. For processes where the projected rejection rates are highly uncertain, the capsule cost was determined at more than one rejection rate.

A few techniques were used to estimate equipment costs. When possible, inflation-adjusted cost of similar equipment that was either previously made or purchased was used. For general process equipment (tanks, etc.), tables (1) giving typical relationships between equipment cost and capacity were utilized. For other items, such as supercritical CO_2 dryers, budgetary quotes were obtained from vendors. The cost of some items, such as laser drilling equipment, was projected based on the upcoming expiration of key patents that will reduce equipment cost over time.

A multiple factor method based on the work of D.R. Woods (2) was used to determine the total fixed capital investment cost. This method uses various factors to determine the costs of piping, electrical, instruments, buildings and auxiliaries, field expenses, engineering, contractor's fees and overhead, and contingency from the cost of the delivered equipment. The factors for this method were selected assuming a grass-roots plant with solids-fluids processing (capsule generation methods using the droplet generator) or a grass-roots plant with solids processing (injection molding).

Operating expenses, consisting of labor, maintenance, materials, and utilities, were then calculated. Staff requirements were determined based on process complexity. For example, for capsules where GDP coating was used in addition to capsule generation via a droplet generator, extra technicians were allocated. Five shifts were assumed for around-the-clock operation. Total labor costs were calculated based on 100% burdening to cover benefits, overhead, and other expenses.

Materials costs were determined from chemical costs and the materials balance, which gives the required chemical flow rates. Chemical costs were compiled, where possible, based on historical bulk price averages. When multiple quotes were available for the same material at different quantities, a curve was made and the value of the curve at the desired quantity was used as the chemical cost. Annual maintenance costs were assumed to be a fixed percentage (6%) of the total capital expenditure.

Financing calculations were performed according to calculations in the publication by Delene et al. (3). A 30 year plant life was assumed along with an inflation rate of 5%.

References:

1. R.H. Perry, D.W. Green, *Perry*'s *Chemical Engineers' Handbook*. 7th ed., Sec. 9, McGraw- Hill, New York, 1997.
2. D.R Woods, *Financial Decision Making in the Process Industry*, Prentice Hall, Englewood Cliffs, NJ (1975).
3. J. G. Delene, K. A. Williams, and B. H. Shapiro, "*Nuclear Energy Cost Data Base.*" U.S. Department of Energy report DOE/NE-0095 (1988).

Thick PAMS:

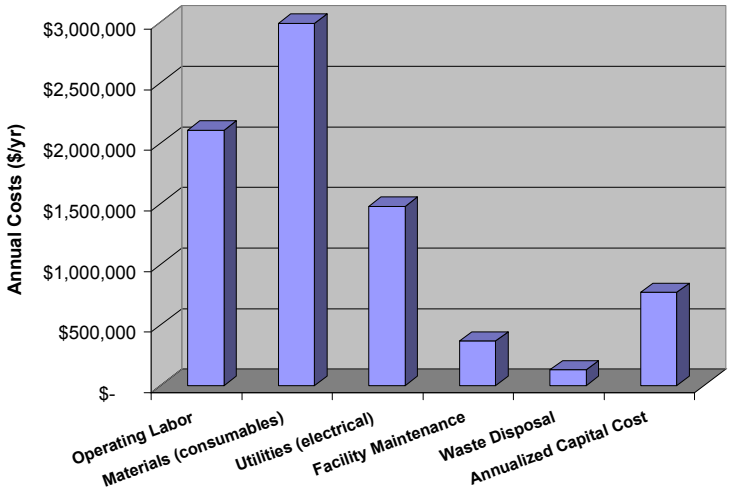

Thin PAMS, GDP coating:

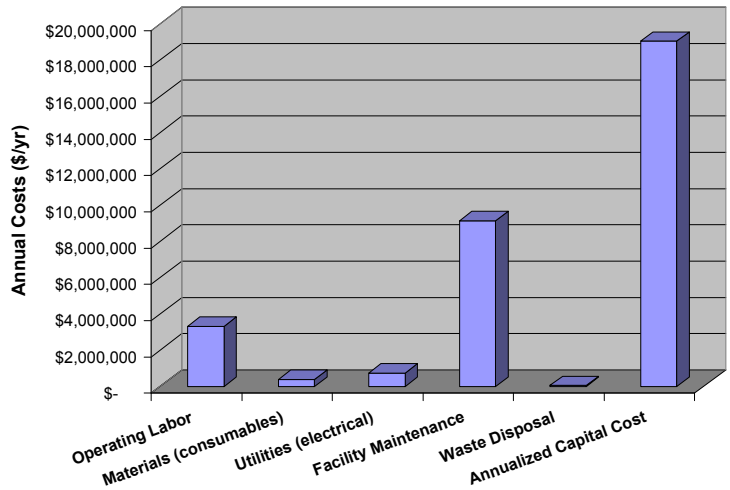

DVB foam, interfacial layer, GDP coating

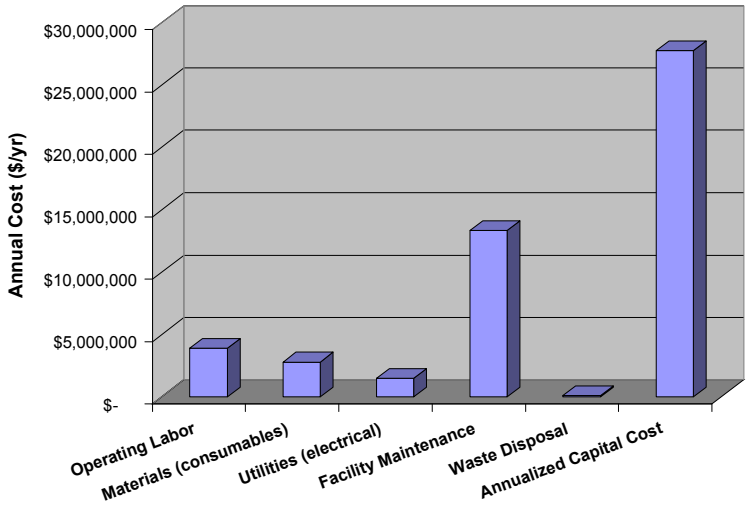

Injection Molding: